Molecular Pharmacology Fast Forward. Published on July 11, 2012 as DOI: 10.1124/mol.112.080291

MOL #80291

Synthesizing Selective Agonists for the α7 Nicotinic Receptor with *in situ* Click-Chemistry on Acetylcholine Binding Protein Templates

John G. Yamauchi, Kimberly Gomez, Neil Grimster, Mikael Dufouil, Ákos Nemecz, Joseph R. Fotsing, Kwok-Yiu Ho, Todd T. Talley, K. Barry Sharpless, Valery V. Fokin, Palmer Taylor

Department of Pharmacology, Skaggs School of Pharmacy & Pharmaceutical Sciences, University of California, San Diego, La Jolla, CA 92093-0657, J.G.Y., K.G., M.D., A.N., K.H., T.T.T., P.T.

Skaggs Institute for Chemical Biology, The Scripps Research Institute, 10550 North Torrey Pines Road, La Jolla, San Diego, CA 92037, N.G., M.D., J.R.F., K.B.S., V.V.F.

Department of Chemistry and Biochemistry, University of California, San Diego, La Jolla, CA 92093-0657, A.N.

Molecular Pharmacology Fast Forward. Published on July 11, 2012 as DOI: 10.1124/mol.112.080291
This article has not been copyedited and formatted. The final version may differ from this version.

Running Title: *Nicotinic Click-Chemistry and Pharmacology*

Corresponding Author information: Palmer Taylor, pwtaylor@ucsd.edu; (858)-534-4028 (tel); (858)-822-5591 (fax); Pharmaceutical Sciences Building, University of California, San Diego 9500 Gilman Drive, La Jolla, CA 92093-0657

Number of Text Pages: 37

Number of Tables: 3

Number of Figures: 2 Schemes and 6 Figures

Number of References: 45

Number of Words in Abstract: 241

Number of words in Introduction: 735

Number of words in Discussion: 1874

Abbreviations List:

5-HT, 5-hydroxytrypamine; *Ac*, *Aplysia californica*; AChBP, acetylcholine binding protein; aCSF, artificial cerebral spinal fluid; *Ac*-MT2, *Ac*-AChBP mutant 2; CNiFER, cell-based neurotransmitter fluorescently engineered reporter; CNS, central nervous system; CuAAC, copper catalyzed azide-alkyne cycloaddition; DHβE, dihydro-beta-erythroidine; DMEM, Dulbecco's modified eagle medium; DMSO, Dimethylsulfoxide; DPBS, Dulbecco's Phosphate Buffered Saline; DR, dose-response; FRET, Förster Resonance Energy Transfer; LC/MS-SIM, liquid chromatography mass spectrometry single ion mode; *Ls*, *Lymnaea stagnalis*; MeCN, acetonitrile, MLA, methyllycaconitine; nAChR, nicotinic acetylcholine receptor; NaN_3, sodium azide pLGIC, pentameric ligand-gated ion channel; RuAAC, ruthenium catalyzed azide-alkyne cycloaddition; TFA, trifluoroacetic acid

Molecular Pharmacology Fast Forward. Published on July 11, 2012 as DOI: 10.1124/mol.112.080291
This article has not been copyedited and formatted. The final version may differ from this version.

Abstract

The acetylcholine binding proteins (AChBPs), which serve as structural surrogates for the extracellular domain of nicotinic acetylcholine receptors (nAChRs), were used as reaction templates for *in situ* click-chemistry reactions to generate a congeneric series of triazoles from azide and alkyne building blocks. The recent achievement of catalyzing *in situ* azide-alkyne cycloaddition reactions at a dynamic subunit interface facilitates synthesis of potentially selective compounds for nAChRs. We investigate compound sets generated *in situ* at soluble AChBP templates with receptor targets through their pharmacological characterization at α7 and α4β2-nAChRs as well as 5-HT_{3A} receptors. Analysis of activity differences between (1,5)-*syn* and (1,4)-*anti* triazole isomers showed a preference towards the (1,4)-*anti* triazole regioisomer among nAChRs. To improve nAChR subtype selectivity, the highest potency building block for α7-nAChRs, 3α-azido *N*-methylammonium tropane, was utilized for additional *in situ* reactions using a mutated *Aplysia californica* AChBP, made to resemble the ligand binding domain of the α7-nAChR. Fourteen of fifty possible triazole products were identified and their corresponding tertiary analogues synthesized. Pharmacological assays revealed that the mutated binding protein template provided enhanced selectivity of ligands through *in situ* reactions. Discrete trends in pharmacological profiles are evident with most compounds emerging as α7-nAChR agonists and α4β2-nAChR antagonists. Triazoles bearing quaternary tropanes and aromatic groups were most potent for the α7-nAChR. Pharmacological characterization of the *in situ* reaction products establish that click-chemistry synthesis, guided with surrogate receptor templates, offers novel extensions of fragment-based drug design applicable to multi-subunit ion channels.

Molecular Pharmacology Fast Forward. Published on July 11, 2012 as DOI: 10.1124/mol.112.080291
This article has not been copyedited and formatted. The final version may differ from this version.

Introduction

Cys-loop receptors are pentameric ligand gated ion channels (pLGICs) defined by two extracellular disulfide linked cysteine residues. Other family members include the 5-hydroxytryptamine type 3 (5-HT_3), γ-aminobutyric acid ($GABA_A$), $GABA_C$, glycine, and invertebrate glutamate and histamine receptors (Karlin, 2002). The nAChRs are activated by the excitatory neurotransmitter, acetylcholine, and are located at synapses in the CNS, neuromuscular junctions, and peripheral autonomic ganglia. They are widely distributed in brain mediating functions such as motor and autonomic activity, memory, and cognitive perceptions.

The α7 and α4β2-nAChRs on pyramidal and interneurons of the hippocampus contribute to synaptic plasticity, memory, and learning by regulating release of excitatory (glutamate) and inhibitory (GABA) neurotransmitters (Kenney and Gould, 2008). Extensive associations with cholinergic neurotransmission in neurodegenerative and developmental diseases have deemed nAChRs as pharmaceutical targets for CNS disorders (Kenney and Gould, 2008; Mudo et al., 2007; Picciotto and Zoli, 2008). The two most abundant subtypes in the brain, α7 and α4β2-nAChRs, have been targeted for development of selective orthosteric and allosteric therapeutic ligands for treatment of Alzheimer's disease, schizophrenia, Parkinson's disease, and for promoting smoking cessation (Taly et al., 2009). Obtaining subtype selective ligands for nAChRs has been challenging due to the multiplicity of receptor subtypes and their discrete CNS locations (Millar and Gotti, 2009).

Azide-alkyne click-chemistry involves highly exergonic biorthogonal cycloaddition reactions to form five membered 1,2,3-triazoles in either the (1,4)-*anti* or (1,5)-*syn* isomer conformation (Scheme 1). The triazole moiety formed is stable and largely resistant to degradation and metabolism (Kolb and Sharpless, 2003). The basicity of the N2 and N3 atoms of 1,2,3-triazoles

Molecular Pharmacology Fast Forward. Published on July 11, 2012 as DOI: 10.1124/mol.112.080291
This article has not been copyedited and formatted. The final version may differ from this version.

is sufficiently low (pKa's of conjugate acids 1.5-2.0) ensuring they remain uncharged at physiological pH values. Yet the triazole ring exhibits a relatively strong dipole moment of ~5 Debye (Purcell and Singer, 1967), and the N2 and N3 atoms serve as weak hydrogen bond acceptors. Triazoles formed in cycloaddition reactions may be regarded as small spacer rings, in which inter-site distances can be controlled by the regioisomer formed through linear linkers between the azide or alkyne.

Freeze-frame click-chemistry, with a flexible target template, carries an advantage of reactant building blocks selecting a conformation preferred by the reaction product, yielding a conformation specific to the bound ligand state. Contemporary drug discovery has encompassed fragment-based drug design; moreover, *in situ* freeze-frame click-chemistry allows the target of drug action to serve as the template. Earlier successful applications of generating lead compounds with *in situ* click-chemistry were on enzyme templates: acetylcholinesterase (Lewis et al., 2002), carbonic anhydrase (Mocharla et al., 2004), and HIV protease (Whiting et al., 2006). The enzyme templates contain sequestered and often deep, active-site pockets to stabilize association of azide and alkyne building blocks and facilitate the cycloaddition reaction.

We were interested in expanding *in situ* click-chemistry on templates of pharmacologically relevant neurotransmitter receptors; such as the nAChR and its Cys-loop cousins. However, performing these reactions with native receptors presents a challenge of template and product isolation in membrane environments, as well the product conforming to an inter-subunit binding site, that typically exhibits cooperative interactions. Using soluble surrogates of the extracellular domain of nAChR subunits, the acetylcholine binding proteins (AChBPs) from *Lymnaea stagnalis* (*Ls*) (Brejc et al., 2001; Smit et al., 2001) and *Aplysia californica* (*Ac*) (Hansen et al., 2004), we generated *in situ* azide-alkyne cycloaddition products at the orthosteric site between

Molecular Pharmacology Fast Forward. Published on July 11, 2012 as DOI: 10.1124/mol.112.080291
This article has not been copyedited and formatted. The final version may differ from this version.

subunit interfaces of these oligomeric proteins, with dissociation constants extending to low nanomolar ranges (Grimster et al., 2012). The azide and alkyne components forming triazoles are mass identified by LCMS. Subsequently, identified regioisomers are synthesized in larger amounts for the *anti* regioisomers, using Cu(I) catalyzed azide-alkyne cycloaddition (CuAAC) (Rostovtsev et al., 2002; Tornoe et al., 2002), and the *syn* regioisomers, using Ru(II) catalyzed azide-alkyne cycloaddition (RuAAC) (Majireck and Weinreb, 2006; Zhang et al., 2005). Since *in situ* 1,2,3-triazole cycloaddition reactions potentially yield (1,4)-*anti* and (1,5)-*syn* regioisomer products, both isomers were synthesized individually in absence of the template (Scheme 2).

Herein, we characterize pharmacological selectivity of previously reported *in situ* click-chemistry lead compounds generated on soluble *Ls*, *Ac,* and *Ac*-Y55W AChBPs (Grimster et al., 2012) with α7 and α4β2-nAChRs, as well as 5-HT_{3A} pLGICs (Scheme 1). Furthermore, we employ a mutated *Ac*-AChBP template (Nemecz and Taylor, 2011), showing greater sequence identity to the α7-nAChR, to synthesize compounds more selective for the α7-nAChR. Our extension of *in situ* click-chemistry to the pLGIC class of membrane bound receptors expands reaction diversity and candidate-lead applications to other targeted receptor systems.

Molecular Pharmacology Fast Forward. Published on July 11, 2012 as DOI: 10.1124/mol.112.080291
This article has not been copyedited and formatted. The final version may differ from this version.

Methods and Materials

Cell lines and AChBP Purification

Cells were cultured in 10cm plates with Dulbecco's modified Eagle medium (Mediatech, Manassas, VA) supplemented with 10% fetal bovine serum (Gemini Bio-Products, West Sacramento, CA) and 1% glutamine (Invitrogen), incubated at 37^{o}C with 10% CO_2. Cell-based neurotransmitter fluorescently engineered reporter (CNiFER) stable cell lines expressing either human α7-nAChR with RIC3 (Human embryonic kidney (HEK) tsA201), human α4β2-nAChR (HEKtsA201), or mouse 5-HT_{3A} serotonin receptors (HEK293) were prepared as documented in (Yamauchi et al., 2011). Each CNiFER cell line contained the genetically encoded Ca^{2+} sensor TN-XXL (Mank et al., 2008) to measure Ca^{2+} flux through the pLGICs. Cells expressing α4β2-nAChRs presumably contained both subtype stoichiometries as described in (Kuryatov et al., 2005). AChBP purification and expression of *Ls*, *Ac*, *Ac*-Y55W, and *Ac*-MT2 AChBPs were performed as previously described (Hansen et al., 2005; Nemecz and Taylor, 2011; Talley et al., 2006). Briefly, amino-terminal FLAG tagged AChBPs were expressed in stable cell lines of HEK293S cells lacking the *N*-acetyglucosaminyltransferase I ($GnTI^{-}$) gene (Reeves et al., 2002). Protein was purified with FLAG-antibody resin and FLAG peptide (Sigma). Pentameric assembly was assessed with size exclusion chromatography in a Superose 6 10/300 GL column (GE Healthcare) in 50 mM Tris-HCl (pH 7.4), 150 mM NaCl, 0.02% NaN_3. Purified AChBP pentamers were concentrated (Millipore) to a final concentration of 5 mg/ml.

Flex Assays with CNiFER Cells

The CNiFER assay identified and characterized compounds as agonists or antagonists by peak FRET responses mediated via Ca^{2+} flux through the pLGICs (Yamauchi et al., 2011). Briefly, tissue-culture treated 96-well plates (E&K, Greiner Campbell, CA) were treated by incubating

Molecular Pharmacology Fast Forward. Published on July 11, 2012 as DOI: 10.1124/mol.112.080291
This article has not been copyedited and formatted. The final version may differ from this version.

wells with 50 μL of 0.1 mg/mL poly-D-lysine (Sigma-Aldrich) for thirty minutes and then washed with Dulbecco's phosphate buffered saline (Mediatech, Manassas, VA). Cells were then plated into the 96-well plates a day prior to assay, and incubated at 37^{o}C with 10% CO_2. Media was replaced with 100 μL of artificial cerebral spinal fluid (aCSF) buffer, including specified antagonists or positive allosteric modulators depending upon assay, and incubated at 37°C for ~30 minutes prior to measuring responses. All aCSF buffers for assays performed with α7-nAChRs contained 10-15 μM PNU-120596 (Tocris, Ellisville, MO). A FlexStation III (Molecular Devices) was used to inject compounds and measure fluorescent responses. A mean EC_{50} value per agonist was calculated from an $n \geq 3$. A set of varied antagonist concentrations were used to measure competitive and non-competitive inhibition, and referenced against a control agonist concentration-response curve. The potencies of competitive antagonists (K_A) were calculated using the Schild analysis (Arunlakshana and Schild, 1959; Wyllie and Chen, 2009) of dose ratios (DR) or with the linear relationship $K_A = [A]/(DR-1)$, where [A] is the antagonist concentration (Taylor and Insel, 1990). The constants of non-competitive antagonists (K_A) are defined as $IC_{50} = K_A$ and were calculated using the equation $K_A = [A]/((\Delta_{max}/\Delta) - 1)$, where Δ/Δ_{max} is the fraction of max response. Values are reported as arithmetic means with standard deviations.

Agonist Screens

Basal fluorescence was recorded for thirty seconds, followed by an addition (50 μL per well) of test ligands prepared in buffer at 3x (40 μM) final concentration (13.3 μM). Measurements were made at 3.54 second intervals per emission wavelength over 120 seconds to assess the potential agonist behavior of each ligand. Control wells were used to normalize responses of the test compounds; buffer was used to measure background fluorescence, 0.1 or 1 μM (±)-epibatidine

Molecular Pharmacology Fast Forward. Published on July 11, 2012 as DOI: 10.1124/mol.112.080291
This article has not been copyedited and formatted. The final version may differ from this version.

(α7-nAChR and α4β2-nAChR) or 1 μM 5-HT (5-HT_{3A}) was used as agonist references, and 1 μM MLA (α7-nAChR), 10 μM dihydro-β erythroidine (α4β2-nAChR), or 0.1 or 1 μM tropisetron (5-HT_{3A}) was used as antagonist references. Agonist responses were normalized as corrected fractions by subtracting the background fluorescence. Three to four activity screens were performed with three replicates per screen and overall means were calculated with standard deviations from the mean of each screen. Compounds that produced a normalized fractional agonist response of 0.2 or greater were identified as agonists and further characterized with EC_{50} values from concentration-response curves.

Antagonist Screens

Directly following the agonist screen, which takes approximately 25-35 minutes to complete, 50 μL of a reference agonist at the max response concentration (prepared at 4x final) was injected into each well to assess the potential antagonist property of tested compounds (10 μM final). Final concentrations of 0.1 or 1 μM (±)-epibatidine (α7-nAChR or α4β2-nAChR) or 1 μM 5-HT (5-HT_{3A}) were used as agonists to ascertain any inhibition by the test compounds. Responses were normalized as the fraction of antagonist inhibition. The number of screens performed and calculation of values were the same as described in the agonist screens. Compounds that blocked with an inhibition fraction of 0.5 or greater were characterized further to derive K_A values for competitive or non-competitive inhibition.

Radioligand Binding Assays

The AChBP Scintillation Proximity Assay (SPA) was used to determine the apparent K_d value of the compounds as reported previously (Talley et al., 2006). Briefly, AChBP (0.5-1.0 nM final concentration in binding sites), polyvinyltoluene anti-mouse SPA scintillation beads (0.17mg/ml final concentration, Perkin Elmer), monoclonal anti-FLAG M2 antibody from mouse 1:8000

Molecular Pharmacology Fast Forward. Published on July 11, 2012 as DOI: 10.1124/mol.112.080291
This article has not been copyedited and formatted. The final version may differ from this version.

dilution (Sigma), and (±)-[^{3}H]-epibatidine (Perkin Elmer) were combined in 0.1M $NaPO_4$ buffer, pH 7.0. Nonspecific binding was determined in parallel by adding a saturating concentration (12.5 μM) of MLA (Tocris) to an identical set of wells. Competition assays were conducted with a constant concentration of (±)-[^{3}H]-epibatidine (5-20 nM final) for each respective AChBP and varying the concentrations of competing ligand. A minimum of three independent experiments, performed in duplicates, were used to determine the K_d values as the arithmetic mean with standard deviations.

In Situ Synthesis from Azide and Alkyne Libraries

3α-azido *N*-methylammonium tropane was dissolved in 0.1M $NaPO_4$ buffer, pH 7.0 (100 mM). Fifty alkynes (Supplemental Figure 3) were dissolved in dimethylsulfoxide (DMSO) and combined to give a final alkyne concentration of 50 mM. The 3α-azido *N*-methylammonium tropane solution (10 μL) was added to *Ac*-MT2 AChBP (~1 mg/mL in 0.1M $NaPO_4$ buffer, pH 7.0, 980 μL) in a microfuge tube, followed immediately by the combined alkyne solution (10 μL). The reactants were briefly mixed and then incubated at room temperature. In a separate microfuge tube, 3α-azido *N*-methylammonium tropane (10 μL, 100 mM in 0.1M $NaPO_4$ buffer, pH 7.0) and the combined alkyne solution (10 μL, 50 mM in DMSO) were diluted with water (870 μL) before aq. copper sulfate (10 μL, 0.05 M) and aq. sodium ascorbate (100 μL, 0.1M) were added. The reactants were mixed and then incubated at room temperature.

After 10 days, both samples were analyzed, in triplicate, using liquid chromatography-mass spectrometry selected ion monitoring (LC/MS-SIM): Zorbax, 4.6 mm x 3 cm, SB-C18 (rapid resolution) reverse phase column, preceded by a Phenomenex C18 guard column, flow rate 0.5 mL/min, using a gradient elution as follows: (H_2O + 0.05% Trifluoroacetic acid [TFA]):(MeCN + 0.05 % TFA) 100:0 to 0:100 over 15 min; then 100 % MeCN + 0.05 % TFA for 5 min with a

Molecular Pharmacology Fast Forward. Published on July 11, 2012 as DOI: 10.1124/mol.112.080291
This article has not been copyedited and formatted. The final version may differ from this version.

post run time of 5 min using the starting solvent ratio. MS detection was performed by electrospray ionization mass spectrometry using positive selected-ion monitoring. To increase MS detection sensitivity, 10 injections (each 25 μL) were performed; each injection was tuned to detect five of the expected 50 molecular weights. The cycloaddition products of the *in situ* screen were identified by their molecular weights and by comparison of retention times of the formed product with the values determined by analysis of the copper catalyzed reactions. A control experiment, performed as above, substituted bovine serum albumin (1 mg/mL) for *Ac*-MT2 AChBP. LC/MS-SIM analysis detected no triazole products in the presence of bovine serum albumin.

Molecular Pharmacology Fast Forward. Published on July 11, 2012 as DOI: 10.1124/mol.112.080291
This article has not been copyedited and formatted. The final version may differ from this version.

Results

Compounds Generated in situ with Ls, Ac, and Ac-Y55W AChBPs

We were interested initially in investigating functional nAChR activity of compounds (***1-9***), that were identified and generated previously using azide-alkyne *in situ* click-chemistry with *Ls*, *Ac,* and *Ac*-Y55W AChBPs as reaction templates (Grimster et al., 2012). Initially, the (1,4)-*anti* isomers were examined, since they could be synthesized in larger quantities using CuAAC. We were also interested in differences between triazole regioisomers, therefore, we also synthesized the (1,5)-*syn* triazole isomers (***1'-5'***) of compounds ***1-5***. The chemical structures of triazoles ***1-5***, ***1'-5'***, and ***6-9*** are shown in Table 1. Initial data that reveal agonist and antagonist activities or lack thereof at the α7 and α4β2-nAChR, as well as 5-HT_{3A} receptors are shown in Supplemental Figure 1.

Pharmacological tests for the α7-nAChR identified all fourteen triazole compounds as agonists and none as antagonists at 13.3 μM. Notably, (1,4)-*anti* triazoles ***1*** and ***3*** exhibited slightly higher agonist activities (potencies) than the (1,5)-*syn* isomers ***1'*** and ***3'*** (Supplemental Figure 1A). Agonist responses elicited at the α7-nAChR by these compounds were blocked with 1 μM methyllycaconitine (MLA) (Mogg et al., 2002) to establish the responses were specific to the transfected α7-nAChRs (Supplemental Figure 2). The α7-nAChR agonists were characterized with concentration-response curves, and the (1,4)-*anti* isomers showed slightly greater potencies, ranging from 2 to 3 fold for α7-nAChR agonists, except in the case of ***1*** and ***3***, and 2 to 6 fold for α4β2-nAChR competitive antagonists, except in the case of ***1*** (Supplemental Table 1). This general trend also holds true for the (1,4)-*anti* and (1,5)-*syn* triazoles binding to the three AChBPs (Table 1 and Supplementary Table 1). Triazoles ***4*** and ***4'*** exhibited slight differences in K_d (1.0nM and 2 nM) and EC_{50} (0.3 μM and 0.6 μM) for *Ls*-AChBP and α7-nAChR respectively

Molecular Pharmacology Fast Forward. Published on July 11, 2012 as DOI: 10.1124/mol.112.080291
This article has not been copyedited and formatted. The final version may differ from this version.

(both with two-fold activity ratios), whereas substantial differences were seen for *Ac* (24 nM and 300 nM) and *Ac*Y55W (17 nM and 100 nM) AChBPs with activity ratios of 13 and 5.8 respectively (Table 1A and Supplemental Table 1). Triazole ***4*** showed the highest overall affinity for α7-nAChR among the other (1,4)-*anti* compounds tested (Figure 1).

None of the fourteen compounds tested at 13.3 μM were agonists for the α4β2-nAChR, while eight were found to be antagonists at 10 μM (***1-5***, ***6***, ***8***, and ***9,*** Supplemental Figure 1B). A Schild analysis was performed from graded responses derived from incubating various concentrations of the antagonists, 30 minutes before agonist addition to α4β2-nAChR CNiFER cells. The well-characterized α4β2-nAChR antagonists dihydro-beta-erythroidine and mecamylamine produced inhibition profiles with expected competitive and non-competitive characteristics, respectively (Figure 2), and served as reference indicators for types of antagonism.

Measurements of ion permeability over a time course of several seconds incur distortions from possible desensitization and changes in intracellular ion distribution. Nevertheless, the sample throughput allows for multiple measurements of agonist responses and antagonist block by the Schild null method. The approach is particularly useful in distinguishing agonist from antagonist responses and rank ordering potencies across multiple receptor subtypes.

Despite overall structural similarities, the triazole antagonists exhibit a spectrum of apparent mixed competitive and non-competitive inhibition profiles. Triazole ***4*** was the most potent antagonist for the α4β2-nAChR, with a measured competitive K_A value of 4 μM, and 5.8 fold more potent than its (1,5)-*syn* counterpart ***4'***. (Table 1A, Supplementary Table 1, and Figure 3). Although both compounds showed non-competitive characteristics at concentrations above 10 μM, the competitive component was significantly stronger for ***4,*** as seen in the profile of the curves obtained with 3 μM and 10μM (Figure 3A). Compound ***4'*** showed less competitive

Molecular Pharmacology Fast Forward. Published on July 11, 2012 as DOI: 10.1124/mol.112.080291
This article has not been copyedited and formatted. The final version may differ from this version.

inhibition than ***4***, having nearly equal contributions of competitive and non-competitive inhibition as seen in Figure 3B. Overall the competitive components of inhibition were stronger with α4β2-nAChRs than the non-competitive components (Supplemental Table 2). The fourteen compounds tested were all weaker as antagonists on the α4β2-nAChR than as agonists on the α7-nAChR with differences in some cases larger than 10-fold (Table 1 and Supplemental Table 3).

None of the compounds displayed agonist activity when tested against the 5-HT_{3A} receptor at 13.3 μM, and only triazole ***4'*** was found to be an antagonist at 10 μM (Supplemental Figure 1C). The inhibition profile with ***4'*** showed competitive blocking of 5-HT elicited responses with a calculated competitive K_A value of 0.9 μM (Figure 4A). Interestingly, its (1,4)-*anti* triazole isomer ***4*** was found to be a much weaker 5-HT_{3A} antagonist with a competitive K_A value of 34 μM (Figure 4C), which translates to a 38-fold higher potency of inhibition for the (1,5)-*syn* isomer ***4'***. Compared to the α7 and α4β2-nAChRs, which prefer the (1,4)-*anti* compounds, the 5-HT_{3A} receptor showed a preference for the *N*-methylammonium tropane (1,5)-*syn* triazole ***4'*** over its (1,4)-*anti* counterpart ***4*** in the only instance where activity was seen. (Table 1A and Supplemental Table 1).

In addition to receptor activities, Table 1A compares AChBP binding values previously reported in Grimster, N. *et. al.* 2012 for analysis of the (1,4)-*anti* (***1-5***) vs (1,5)-*syn* triazoles (***1'-5'***) as well as containing triazole ***6***, an initial product formed with the AChBPs (Grimster et al., 2012). The tested receptor and AChBP activities of the synthesized quaternary amine (1,4)-*anti* triazoles (***7-9***), also generated by *in situ* synthesis (Grimster et al., 2012), are shown in Table 1B. All four of the compounds (***6-9***) were found to be moderately potent agonists for the α7-nAChR with

Molecular Pharmacology Fast Forward. Published on July 11, 2012 as DOI: 10.1124/mol.112.080291
This article has not been copyedited and formatted. The final version may differ from this version.

comparable EC_{50} values to those seen in ***1-5***. Compounds ***6***, ***8***, and ***9*** were weak to moderate antagonists at α4β2-nAChRs, whereas none (***6-9***) were active at the 5-HT_{3A} receptor.

Compounds generated with a partial α7/Ac-AChBP chimera

The initial *in situ* generated compounds (***1-5***, ***1'-5'***, and ***6-9*** in Table 1 and Supplemental Table 3) indicated that AChBPs might serve as promising templates for the generation of candidate ligands selective at α7-nAChRs. To find selective and more potent compounds for the α7-nAChR, we performed an additional round of *in situ* click-chemistry reactions, but utilized *Ac*-MT2 (Nemecz and Taylor, 2011), an available *Ac*-AChBP mutant that had residues in the binding site mutated towards the human α7-nAChR. To obtain *Ac*-MT2, mutations were made in the *Ac*-AChBP at loops B, D, and E, but not at loop C.

Among the above set of 14 compounds, ***4*** and ***4***' were determined to be the most potent for the α7-nAChRs and contained the 3α-azido *N*-methylammonium tropane building block moiety. Thus, we utilized this azide building block to maintain potency for the α7-nAChR, and screened 50 alkyne constituents to develop new selective triazoles (Supplemental Figure 3). Since (1,4)-*anti* isomers typically exhibited lower EC_{50} values for the α7-nAChR, and the (1,5)-*syn* isomer (***4'***) showed stronger inhibition of the 5-HT_{3A} receptor than the (1,4)-*anti* isomer (***4***), CuAAC was used to synthesize only the (1,4)-*anti* isomers of the compounds generated *in situ* upon *Ac*-MT2.

Of the 50 alkyne building blocks that were reacted *in situ* with 3α-azido *N*-methylammonium tropane using *Ac*-MT2 as a template, a total of 14 triazole products were identified and subsequently synthesized using CuAAC (***10^q-23^q***). Pharmacological profiles for the assayed receptors are shown in Table 2. All 14 compounds were identified as MLA sensitive agonists for the α7-nAChR (Supplemental Figure 4A and 5) with ***13^q***, ***15^q***, ***17^q***, ***18^q***, and ***22^q***, exhibiting EC_{50}

Molecular Pharmacology Fast Forward. Published on July 11, 2012 as DOI: 10.1124/mol.112.080291
This article has not been copyedited and formatted. The final version may differ from this version.

values less than 1 μM (Table 2). The quaternary 2-(methylthio)-benzothiazole triazole (***15^q***) had the highest affinity for the α7-nAChR (EC_{50} = 0.20 μM). For the α4β2-nAChR, ***15^q*** was an antagonist, but with 15 fold weaker antagonist activity revealing its α7 selectivity (competitive K_A = 3 μM and non-competitive K_A = 8 μM) (Supplementary Table 4). All of the fourteen quaternary compounds showed the trend of selectivity for the α7-nAChR, although ***20^q*** and ***23^q*** showed a mere 3.8 fold selectivity, and ***11^q***'s weak potency rendered minimal selectivity of at least three-fold. The 1-(2-methoxynapthalene)-ethanone (***22^q***) triazole was selected as a good lead compound based on its selectivity and potency (EC_{50} = 0.4 μM) for α7-nAChRs. Triazoles ***13^q***, ***15^q***, ***17^q***, and ***18^q*** were α4β2-nAChR antagonists of moderate activity, with competitive K_A values less than 10 μM, whereas ***19^q***, ***20^q***, ***21^q***, and ***23^q*** were found to weakly antagonize α4β2-nAChRs. Interestingly, triazoles ***15^q***, ***17^q***, and ***18^q*** had similar near-equivalent competitive and non-competitive K_A values that were less than 10 μM. Of the fourteen triazoles ***17^q*** was the only compound identified as an antagonist for the 5-HT_{3A} receptor and showed a dominant non-competitive antagonism profile with a K_A of 8 μM (Figure 5B).

To assess the role of the quaternization of the aza nitrogen in α7-nAChR activation, the corresponding tertiary free amine analogue of ***4*** (***4^t***) and the 14 above mentioned 3α-azido *N*-methylammonium tropane derivatives (***10^t-23^t***) were synthesized and subsequently investigated for functional and binding activity against the receptors and AChBPs respectively (Table 3). Only five of the fifteen tropane triazole products (***4^t***, ***15^t***, ***16^t***, ***20^t***, ***22^t***) were found to be agonists for α7-nAChRs, as all tertiary analogues lost significant affinity with none having an EC_{50} value below 1 μM. Compound ***16^t***, however, did maintain 6-fold selectivity for α7-nAChRs. Interestingly, an increase in affinity was found for most of the tertiary analogues against α4β2-nAChRs with ***10^t***, ***12^t***, ***14^t***, and ***16^t*** displaying weak antagonism whereas their quaternary

Molecular Pharmacology Fast Forward. Published on July 11, 2012 as DOI: 10.1124/mol.112.080291
This article has not been copyedited and formatted. The final version may differ from this version.

counterparts displayed no appreciable antagonism. Triazole ***13^t*** switched the dominant mechanism of action from a competitive to non-competitive mode of inhibition, whereas ***21^t*** switched from non-competitive to competitive, and both increased overall potency. Triazoles ***15^t*** and ***18^t*** maintained moderate antagonism and behavior for α4β2-nAChRs, with ***22^t*** increasing its affinity to behave similarly as ***15^t*** and ***18^t*** with near-equivalent measured competitive and non-competitive K_A values at less than 10 μM. Triazole ***20^t*** and ***23^t*** also maintained their behavior displaying a similar weak antagonism, whereas triazoles ***4^t***, ***17^t*** and ***19^t*** were the only triazoles to lose affinity for α4β2-nAChRs. There were also more tertiary than quaternary triazole compounds that were active at the 5-HT_{3A} receptor (Supplementary Table 4); these typically were higher in potency and showed competitive inhibition profiles as shown in Figure 5A. The tertiary compounds identified as antagonists for the 5-HT_{3A} receptor were ***4^t***, ***13^t***, ***15^t***, ***18^t***, and ***22^t***. Changing the tertiary tropane amine to a quaternary amine affected the non-competitive component significantly for the 5-HT_{3A} receptor, whereas the weak competitive component was hardly affected (Table 3). The tertiary analogues, ***13^t*** and ***22^t*** created moderate competitive inhibition of 5-HT_{3A} receptors (Figure 5A). However, for ***15^t*,** competitive inhibition was less pronounced. Triazole ***18^t*** had weak but similar near-equivalent competitive and non-competitive components of inhibition on the 5-HT_{3A} receptor (Figure 5B, Table 3).

Molecular Pharmacology Fast Forward. Published on July 11, 2012 as DOI: 10.1124/mol.112.080291
This article has not been copyedited and formatted. The final version may differ from this version.

Discussion

In situ Click-chemistry Generated Leads

From this study, along with a previous analysis (Grimster et al., 2012), we establish that *in situ* click-chemistry can be employed to generate new leads for pharmacological receptors using surrogate AChBPs as soluble templates for synthesis. Hence, template applicability is expanded from well-defined and partially sequestered sites within enzyme subunits to a subunit interface on a multi-subunit protein.

In contrast to traditional fragment-based drug design, the *in situ* approach allows the target template to drive synthetic preferences by selecting combinations of building blocks that best occupy the active site; this was demonstrated with a minimal set using acetylcholinesterase (Lewis et al., 2002) and now by employing AChBP for more diverse building block arrays. The amount of product formed *in situ* correlated with the overall affinity of the complex formed on the target surface (Grimster et al., 2012). Through previous work (Bourne et al., 2004; Bourne et al., 2010b; Lewis et al., 2002), *in situ* click-chemistry was shown to select minor abundance conformations that have a higher affinities for the generated triazole than the predominant unliganded conformation. Hence, the click-chemistry reaction freezes in-frame template conformations preferring formation of the complex. However, this conformational selection is based solely on ligand affinity and does not distinguish agonist from antagonist activity.

Selectivity for the nAChRs and the AChBPs

Our functional LGIC receptor studies with α7-nAChR lead compounds, generated *in situ* with different AChBP templates, reveal findings critical to ever-expanding applications of *in situ* click-chemistry, and identify ligand determinants conferring α7-nAChR selectivity. First, from previously generated *in situ* compounds (***1-9***, ***1'-5'***), we identified the (1,4)-*anti* triazole as the

Molecular Pharmacology Fast Forward. Published on July 11, 2012 as DOI: 10.1124/mol.112.080291
This article has not been copyedited and formatted. The final version may differ from this version.

preferred regioisomer for the α7-nAChR, because of its observed potency and lack of 5-HT_{3A} receptor activity, evident with (1,5)-*syn* isomer triazole ***4'*** (Table 1). Then, we chose a lead azide building block, the 3α-azido *N*-methylammonium tropane (Grimster et al., 2012), because triazole ***4*** had the highest α7-nAChR affinity (Table 1).

We hypothesized that the products formed on the *Ac*-MT2 template (Nemecz and Taylor, 2011), that more closely replicates α7-nAChR, would exhibit enhanced α7-nAChR affinity and thus confer additional selectivity. Chemical refinement of the alkyne termini resulted in 14 triazole products (***10^q-23^q***) forming from 50 alkyne building blocks (Supplementary Figure 4) allowed to react *in situ* with the 3α-azido *N*-methylammonium tropane. All 14 products were functionally selective as α7-nAChR agonists; with five exhibiting EC_{50} values below 1 μM (***13^q***, ***15^q***, ***17^q***, ***18^q***, and ***22^q***), while eight (***13^q***, ***15^q***, ***17^q***, ***18^q***, ***19^q***, ***20^q***, ***21^q*** and ***23^q***) showed α4β2 antagonism. Remarkably, 11 of the 14 triazoles generated were five-fold or more selective for the α7-nAChR (***11^q***, ***20^q***, and ***23^q*** being the exceptions, where ***11^q*** had poor affinity limiting the selectivity determination) and one, ***22^q*,** was both potent and at least seventy-five fold selective (Table 2, Supplementary Table 4). The quaternary *in situ* agonists for α7-nAChRs showed greater selectivity relative to 5-HT_{3A} receptors than α4β2-nAChRs (Supplementary Table 4), an expectation arising from higher conservation of aromatic residues in the nAChR binding site.

Our comparison of tertiary (***4^t*** and ***10^t-23^t***) and quaternary (***4*** and ***10^q-23^q***) (1,4)-*anti* triazoles shows large reductions in α7-nAChR activity by replacing the quaternized nitrogen. Five of the tertiary amine analogues (***4^t***, ***15^t***, ***16^t***, ***20^t***, and ***22^t***) were detected as α7-nAChR agonists but none were highly selective (Supplementary Table 6). The lower activity of these tertiary tropane triazoles presents a limitation, because a fractional unprotonated (neutral) amine species is required to cross the blood-brain barrier as a candidate CNS therapeutic. However, quaternary

Molecular Pharmacology Fast Forward. Published on July 11, 2012 as DOI: 10.1124/mol.112.080291
This article has not been copyedited and formatted. The final version may differ from this version.

compounds offer unique therapeutic opportunities to target α7-nAChRs outside the CNS, such as controlling peripheral inflammation (de Jonge and Ulloa, 2007).

All products were α7-nAChR agonists and contained the aza nitrogen moiety of the *N*-methylammonium tropane, as well as short linkers to either an aromatic or aliphatic group with weak hydrogen bond acceptor capacity. The most potent and selective compound, triazole ***22[q]***, features a positively charged *N*-methylammonium tropane and aromatic methyleneoxynapthylenethanone. Our other products formed reveal pharmacophore models for leads consistent with studies on α7-nAChRs (Horenstein et al., 2008), demonstrating the recognition capacity of the template to select preferred binding partners.

Structural Insights into α7-nAChR Selectivity from AChBP

The most potent triazoles for the α7-nAChR were the *N*-methylammonium tropane (1,4)-*anti* triazoles and given the structural similarities among them, all compounds are predicted to bind in a similar pose to a common receptor or binding protein as shown in the *Ac*-AChBP complex with ***4*** (Figure 6), referred to as "***18***" (PDB: 4DBM) in (Grimster et al., 2012). This structure reveals potential cation-π interactions (Dougherty, 1996) between the quaternary nitrogen and the π-orbitals of a nest of aromatic side chains in the receptor binding-pocket (Blum et al., 2010; Puskar et al., 2011; Xiu et al., 2009) as a dominant contributor to the stability of the complex (Figure 6A). The complement of α subunit aromatic side chains Try 93, Trp 147, Tyr 188, and Tyr 195, in addition to Tyr or Trp 55 on the complementary face are all conserved in AChBPs, and in α7 and α4β2-nAChRs.

Stabilization of tertiary amine complexes differ where stabilization is conferred through a protonated amine and donating a hydrogen bond to the backbone carbonyl group of Trp 147 as reported in AChBP complexes of nicotine PDB:1UW6 (Celie et al., 2004), epibatidine

Molecular Pharmacology Fast Forward. Published on July 11, 2012 as DOI: 10.1124/mol.112.080291
This article has not been copyedited and formatted. The final version may differ from this version.

PDB:2BYQ (Hansen et al., 2005), and the tertiary tropane, tropisetron PDB: 2WNC (Hibbs et al., 2009). A similar situation arises for protonated imines in anabaseine analogues and macrocyclic dinoflagelate toxins (Bourne et al., 2010a; Hibbs et al., 2009). The protonated nitrogen is appropriately oriented within hydrogen bonding distances (2.9-3.1 Å) from the amide backbone carbonyl of Trp 147. The structures reveal a 1.2 Å (4.2 vs 3.0 Å) difference between the quaternary and tertiary nitrogen positions of the tropane amines (Figure 6A).

However, in the presumed binding site at the subunit interface of the 5-HT_{3A} receptor, Tyr 93 is replaced by Asn and Tyr 188 by Ile (Figure 6A). Moreover, the complementary subunit face possesses an increase in aromatic side chains (Tyr 106, Tyr 108, and Tyr 118) not found in AChBPs or nAChRs. This altered position of aromatic side chains, may explain the 5-HT_{3A} preference of tertiary over quaternary tropanes and may suggest an inverted ligand pose.

The triazole ring is found to be partially occluded with its ring carbons facing outward of the pore towards the vicinal Cys 190 and 191 in loop C (Figure 6A). The triazole nitrogen N3 of ***4*** is oriented toward the complementary subunit occupying positions identical to the pyridine nitrogens in epibatidine and nicotine including the formation of a hydrogen bond to a water molecule (Figure 6C). The overlay of the third ring system shows a major departure of positioning of the quinolinone ring in ***4*** and the indole ring in tropisetron.

Our functional studies with the triazole compounds revealed two response modes between nAChR subtypes: agonists for the α7-nAChR and antagonists for the α4β2-nAChR. Studies of Dougherty and Lester using unnatural amino acids also found that these receptors reveal different energy contributions among the aromatic side chains (Blum et al., 2010; Puskar et al., 2011; Xiu et al., 2009). A stronger cation-π interaction at Trp 147 is evident for α4β2-nAChR sites than for α7-nAChR sites, whereas the α7-nAChR site forms a strong cation-π interaction at

Molecular Pharmacology Fast Forward. Published on July 11, 2012 as DOI: 10.1124/mol.112.080291
This article has not been copyedited and formatted. The final version may differ from this version.

Tyr 195. Also the strength of the hydrogen bond formed at the backbone carbonyl of Trp 147 is strong for α4β2-nAChRs but moderate for α7-nAChRs, explaining the tertiary preference for α4β2-nAChRs. These results along with our findings of distinct agonist (α7-nAChR) and antagonist (α4β2-nAChR) actions of the *N*-methylammonium tropane triazoles reveal clear distinctions in binding modes between the α7 and α4β2-nAChRs and suggest that occupation and activation of nAChRs result from distinct poses of the triazole ligand on α7-α7 than on α4-β2 principal-complementary interfaces.

Refinement of the Leads for Nicotinic Receptors

Leads generated by *in situ* click-chemistry are self-limited by template structure and conformation upon which the triazoles are generated. While possessing shared recognition capacities common for neurotransmitters and an array of peptide, alkaloid, and terpene toxins, the structurally homologous AChBPs and nAChRs reveal several distinct characteristics. First, while AChBPs exist in select invertebrate species (Celie et al., 2005; Hansen et al., 2004; Huang et al., 2009; McCormack et al., 2010; Smit et al., 2001), evolutionary distances impart substantial sequence differences from human nAChRs. Second, ligand binding to AChBP is described by a simple adsorption isotherm and does not show cooperativity seen in the nAChR indicative of multiple protein states (Hansen et al., 2004). Hence, interconversion of conformational states of nAChR governed by the ligand is not evident in AChBP. Third, a refined analysis of selectivity over an increasing range of ligands indicates that AChBPs, similar to the receptor subtypes, have species-specific recognition properties not replicated in a single receptor subtype (Hansen et al., 2005; Hibbs et al., 2009; Rucktooa et al., 2009; Talley et al., 2006).

To overcome the limitations of the AChBP templates for nAChR ligand generation, we considered two approaches to enhance selectively. In a previous study, the *Ac* and *Ls*-AChBPs

Molecular Pharmacology Fast Forward. Published on July 11, 2012 as DOI: 10.1124/mol.112.080291
This article has not been copyedited and formatted. The final version may differ from this version.

were mutated to become more α7-like in sequence particularly around the interfacial binding site (Nemecz and Taylor, 2011). The enhanced selectivity conferred by the modified binding site is nevertheless limited by AChBP folding not tolerating several mutations. Although the α7-nAChR template (*Ac*-MT2) is far from a precise replicate of the receptor target, *in situ* generated products offer insights into the chemical landscape around the template pocket that resembles the α7-nAChR.

A second approach is to examine selectivity in structural terms using congeneric ligands in complex with various AChBPs, particularly with mutants resembling human receptors. As these complexes become available, classification of binding poses with respective chemical groupings of agonists and antagonists may elucidate mechanisms of nAChR selectivity.

We characterized leads, in which heterocyclic amines were modified to identify the 3α-azido *N*-methylammonium tropane as a potent α7-nAChR building block lead. By utilizing the functional receptor assay, rapid determination of pharmacological activities (agonist or antagonist) is possible for LGIC receptors enabling one to rank order potencies of *in situ* leads generated at AChBP templates. A logical extension of *in situ* screening entails refinement through synthetic modifications of identified *in situ* leads, such as triazole ***22***^{q}, to enlarge the ligand base through Cu(I) and Ru(II) catalyzed synthetic reactions.

In summary, click-chemistry with *in situ* generated leads followed by catalytic syntheses presents a novel and efficient tool in drug discovery by decreasing time and materials required to identify chemical space surrounding a protein recognition site. In cases where the drug target is limited by its expression in soluble form, we show soluble surrogates may be used as *in situ* templates, and lead compounds can transition from possessing affinity at the soluble template (AChBP) to agonist/antagonist activity at receptors. We demonstrate here two independent

Molecular Pharmacology Fast Forward. Published on July 11, 2012 as DOI: 10.1124/mol.112.080291
This article has not been copyedited and formatted. The final version may differ from this version.

approaches to address the refinement of structure to enhance selectivity. The first involves conversion of the template through mutagenesis to become more receptor like in sequence, while the second entails catalytic synthesis of congeners of the lead(s). An inherent advantage of a soluble template is the opportunity for structural characterization of the lead-target complexes to define the design base. The potential is not yet fully realized, but as more structures become available, idealizing the template and ligand structure modification should lead to more rigorous design constraints.

Molecular Pharmacology Fast Forward. Published on July 11, 2012 as DOI: 10.1124/mol.112.080291
This article has not been copyedited and formatted. The final version may differ from this version.

Acknowledgements

A special thank you to Jean-Pierre Changeux for insightful and provocative discussions. We acknowledge Wenru Yu for her expertise in tissue culture and protein purification.

Authorship Contributions

Participated in research design: Yamauchi, Grimster, Nemecz, Talley, Sharpless, Fokin, Taylor.

Conducted experiments: Yamauchi, Gomez, Grimster, Dufouil, Fotsing, Ho.

Contributed new reagents or analytic tools: Yamauchi, Grimster, Dufouil, Nemecz, Talley, Sharpless, Fokin, Taylor.

Performed data analysis: Yamauchi, Gomez, Grimster, Dufouil, Nemecz, Fotsing, Ho, Talley, Sharpless, Fokin, Taylor.

Wrote or contributed to the writing of the manuscript: Yamauchi, Grimster, Nemecz, Fotsing, Sharpless, Fokin, Taylor.

Molecular Pharmacology Fast Forward. Published on July 11, 2012 as DOI: 10.1124/mol.112.080291
This article has not been copyedited and formatted. The final version may differ from this version.

References

Arunlakshana O and Schild HO (1959) Some quantitative uses of drug antagonists. *Br J Pharmacol Chemother* **14**(1):48-58.

Blum AP, Lester HA and Dougherty DA (2010) Nicotinic pharmacophore: the pyridine N of nicotine and carbonyl of acetylcholine hydrogen bond across a subunit interface to a backbone NH. *Proc Natl Acad Sci U S A* **107**(30):13206-13211.

Bourne Y, Kolb HC, Radic Z, Sharpless KB, Taylor P and Marchot P (2004) Freeze-frame inhibitor captures acetylcholinesterase in a unique conformation. *Proc Natl Acad Sci U S A* **101**(6):1449-1454.

Bourne Y, Radic Z, Araoz R, Talley TT, Benoit E, Servent D, Taylor P, Molgo J and Marchot P (2010a) Structural determinants in phycotoxins and AChBP conferring high affinity binding and nicotinic AChR antagonism. *Proc Natl Acad Sci U S A* **107**(13):6076-6081.

Bourne Y, Radic Z, Taylor P and Marchot P (2010b) Conformational remodeling of femtomolar inhibitor-acetylcholinesterase complexes in the crystalline state. *J Am Chem Soc* **132**(51):18292-18300.

Brejc K, van Dijk WJ, Klaassen RV, Schuurmans M, van Der Oost J, Smit AB and Sixma TK (2001) Crystal structure of an ACh-binding protein reveals the ligand-binding domain of nicotinic receptors. *Nature* **411**(6835):269-276.

Celie PH, Klaassen RV, van Rossum-Fikkert SE, van Elk R, van Nierop P, Smit AB and Sixma TK (2005) Crystal structure of acetylcholine-binding protein from Bulinus truncatus reveals the conserved structural scaffold and sites of variation in nicotinic acetylcholine receptors. *J Biol Chem* **280**(28):26457-26466.

Celie PH, van Rossum-Fikkert SE, van Dijk WJ, Brejc K, Smit AB and Sixma TK (2004) Nicotine and carbamylcholine binding to nicotinic acetylcholine receptors as studied in AChBP crystal structures. *Neuron* **41**(6):907-914.

de Jonge WJ and Ulloa L (2007) The alpha7 nicotinic acetylcholine receptor as a pharmacological target for inflammation. *Br J Pharmacol* **151**(7):915-929.

Dougherty DA (1996) Cation-pi interactions in chemistry and biology: a new view of benzene, Phe, Tyr, and Trp. *Science* **271**(5246):163-168.

Grimster NP, Stump B, Fotsing JR, Weide T, Talley TT, Yamauchi JG, Nemecz A, Kim C, Ho KY, Sharpless KB, Taylor P and Fokin VV (2012) Generation of Candidate Ligands for Nicotinic Acetylcholine Receptors via In Situ Click Chemistry with a Soluble Acetylcholine Binding Protein Template. *J Am Chem Soc*.

Hansen SB, Sulzenbacher G, Huxford T, Marchot P, Taylor P and Bourne Y (2005) Structures of Aplysia AChBP complexes with nicotinic agonists and antagonists reveal distinctive binding interfaces and conformations. *EMBO J* **24**(20):3635-3646.

Hansen SB, Talley TT, Radic Z and Taylor P (2004) Structural and ligand recognition characteristics of an acetylcholine-binding protein from Aplysia californica. *J Biol Chem* **279**(23):24197-24202.

Hibbs RE, Sulzenbacher G, Shi J, Talley TT, Conrod S, Kem WR, Taylor P, Marchot P and Bourne Y (2009) Structural determinants for interaction of partial agonists with acetylcholine binding protein and neuronal alpha7 nicotinic acetylcholine receptor. *EMBO J* **28**(19):3040-3051.

Horenstein NA, Leonik FM and Papke RL (2008) Multiple pharmacophores for the selective activation of nicotinic alpha7-type acetylcholine receptors. *Mol Pharmacol* **74**(6):1496-1511.

Huang J, Wang H, Cui Y, Zhang G, Zheng G, Liu S, Xie L and Zhang R (2009) Identification and comparison of amorphous calcium carbonate-binding protein and acetylcholine-binding protein in the abalone, Haliotis discus hannai. *Mar Biotechnol (NY)* **11**(5):596-607.

Karlin A (2002) Emerging structure of the nicotinic acetylcholine receptors. *Nature Reviews Neuroscience* **3**(2):102-114.

Kenney JW and Gould TJ (2008) Modulation of hippocampus-dependent learning and synaptic plasticity by nicotine. *Mol Neurobiol* **38**(1):101-121.

Kolb HC and Sharpless KB (2003) The growing impact of click chemistry on drug discovery. *Drug Discov Today* **8**(24):1128-1137.

Kuryatov A, Luo J, Cooper J and Lindstrom J (2005) Nicotine Acts as a Pharmacological Chaperone to Up-Regulate Human a4B2 Acetylcholine Receptors. *Molecular Pharmacology*:1-13.

Lewis WG, Green LG, Grynszpan F, Radic Z, Carlier PR, Taylor P, Finn MG and Sharpless KB (2002) Click chemistry in situ: acetylcholinesterase as a reaction vessel for the selective assembly of a femtomolar inhibitor from an array of building blocks. *Angew Chem Int Ed Engl* **41**(6):1053-1057.

Majireck MM and Weinreb SM (2006) A study of the scope and regioselectivity of the ruthenium-catalyzed [3 + 2]-cycloaddition of azides with internal alkynes. *J Org Chem* **71**(22):8680-8683.

Mank M, Santos AF, Direnberger S, Mrsic-Flogel TD, Hofer SB, Stein V, Hendel T, Reiff DF, Levelt C, Borst A, Bonhoeffer T, Hubener M and Griesbeck O (2008) A genetically encoded calcium indicator for chronic in vivo two-photon imaging. *Nat Methods* **5**(9):805-811.

McCormack T, Petrovich RM, Mercier KA, DeRose EF, Cuneo MJ, Williams J, Johnson KL, Lamb PW, London RE and Yakel JL (2010) Identification and functional characterization

of a novel acetylcholine-binding protein from the marine annelid Capitella teleta. *Biochemistry* **49**(10):2279-2287.

Millar NS and Gotti C (2009) Diversity of vertebrate nicotinic acetylcholine receptors. *Neuropharmacology* **56**(1):237-246.

Mocharla VP, Colasson B, Lee LV, Roper S, Sharpless KB, Wong CH and Kolb HC (2004) In situ click chemistry: enzyme-generated inhibitors of carbonic anhydrase II. *Angew Chem Int Ed Engl* **44**(1):116-120.

Mogg AJ, Whiteaker P, McIntosh JM, Marks M, Collins AC and Wonnacott S (2002) Methyllycaconitine is a potent antagonist of alpha-conotoxin-MII-sensitive presynaptic nicotinic acetylcholine receptors in rat striatum. *J Pharmacol Exp Ther* **302**(1):197-204.

Mudo G, Belluardo N and Fuxe K (2007) Nicotinic receptor agonists as neuroprotective/neurotrophic drugs. Progress in molecular mechanisms. *J Neural Transm* **114**(1):135-147.

Nemecz A and Taylor P (2011) Creating an alpha7 nicotinic acetylcholine recognition domain from the acetylcholine-binding protein: crystallographic and ligand selectivity analyses. *J Biol Chem* **286**(49):42555-42565.

Picciotto MR and Zoli M (2008) Neuroprotection via nAChRs: the role of nAChRs in neurodegenerative disorders such as Alzheimer's and Parkinson's disease. *Front Biosci* **13**:492-504.

Purcell WP and Singer JA (1967) Electronic and Molecular Structure of Selected Unsubstituted and Dimethyl Amides from Measurements of Electric Moments and Nuclear Magnetic Resonance. *Journal of Physical Chemistry* **71**(13):4316-&.

Puskar NL, Xiu X, Lester HA and Dougherty DA (2011) Two neuronal nicotinic acetylcholine receptors, alpha4beta4 and alpha7, show differential agonist binding modes. *J Biol Chem* **286**(16):14618-14627.

Reeves PJ, Callewaert N, Contreras R and Khorana HG (2002) Structure and function in rhodopsin: high-level expression of rhodopsin with restricted and homogeneous N-glycosylation by a tetracycline-inducible N-acetylglucosaminyltransferase I-negative HEK293S stable mammalian cell line. *Proc Natl Acad Sci U S A* **99**(21):13419-13424.

Rostovtsev VV, Green LG, Fokin VV and Sharpless KB (2002) A stepwise huisgen cycloaddition process: copper(I)-catalyzed regioselective "ligation" of azides and terminal alkynes. *Angew Chem Int Ed Engl* **41**(14):2596-2599.

Rucktooa P, Smit AB and Sixma TK (2009) Insight in nAChR subtype selectivity from AChBP crystal structures. *Biochem Pharmacol* **78**(7):777-787.

Smit AB, Syed NI, Schaap D, van Minnen J, Klumperman J, Kits KS, Lodder H, van der Schors RC, van Elk R, Sorgedrager B, Brejc K, Sixma TK and Geraerts WP (2001) A glia-

derived acetylcholine-binding protein that modulates synaptic transmission. *Nature* **411**(6835):261-268.

Talley TT, Yalda S, Ho KY, Tor Y, Soti FS, Kem WR and Taylor P (2006) Spectroscopic analysis of benzylidene anabaseine complexes with acetylcholine binding proteins as models for ligand-nicotinic receptor interactions. *Biochemistry* **45**(29):8894-8902.

Taly A, Corringer P-J, Guedin D, Lestage P and Changeux J-P (2009) Nicotinic receptors: allosteric transitions and therapeutic targets in the nervous system. *Nat Rev Drug Discov* **8**(9):733-750.

Taylor P and Insel PA (1990) Molecular basis of pharmacologic selectivity . Chapter 1, in *Principles of drug action : the basis of pharmacology 3rd Ed* (Pratt WB and Taylor P eds) pp 1-102, Churchill Livingstone, New York.

Tornoe CW, Christensen C and Meldal M (2002) Peptidotriazoles on solid phase: [1,2,3]-triazoles by regiospecific copper(i)-catalyzed 1,3-dipolar cycloadditions of terminal alkynes to azides. *J Org Chem* **67**(9):3057-3064.

Whiting M, Muldoon J, Lin YC, Silverman SM, Lindstrom W, Olson AJ, Kolb HC, Finn MG, Sharpless KB, Elder JH and Fokin VV (2006) Inhibitors of HIV-1 protease by using in situ click chemistry. *Angew Chem Int Ed Engl* **45**(9):1435-1439.

Wyllie DJA and Chen PE (2009) Taking the time to study competitive antagonism. *Br J Pharmacol* **150**(5):541-551.

Xiu X, Puskar NL, Shanata JA, Lester HA and Dougherty DA (2009) Nicotine binding to brain receptors requires a strong cation-pi interaction. *Nature* **458**(7237):534-537.

Yamauchi JG, Nemecz A, Nguyen QT, Muller A, Schroeder LF, Talley TT, Lindstrom J, Kleinfeld D and Taylor P (2011) Characterizing ligand-gated ion channel receptors with genetically encoded Ca2++ sensors. *PLoS One* **6**(1):e16519.

Zhang L, Chen X, Xue P, Sun HH, Williams ID, Sharpless KB, Fokin VV and Jia G (2005) Ruthenium-catalyzed cycloaddition of alkynes and organic azides. *J Am Chem Soc* **127**(46):15998-15999.

Footnotes

Financial Support

This work was supported by the National Science Foundation (NSF) [Grant GK-12 0742551]; and the National Institutes of Health (NIH) [Grants T32 GM-07752, R01-GM18360-39, U01-DA019372, R01-GM087620].

Presentations

This work is part of the thesis of J.G.Y and was presented in a late breaking abstract and poster by J.G.Y. at Experimental Biology 2012 (San Diego, CA).

Reprints sent to

Palmer Taylor, pwtaylor@ucsd.edu

University of California, San Diego

9500 Gilman Dr. MC 0657, La Jolla, CA 92093-0657

Present Addresses

Université Claude Bernard Lyon 1, France, M.D.

Synomyx, 4767 Nexus Centre Dr. San Diego, CA 92121, J.R.F.

Department of Biomedical and Pharmaceutical Sciences, Idaho State University College of Pharmacy, Pocatello, Idaho 83209-8288, T.T.T.

Supporting Information Available

Additional information is available as supplemental information including; details of synthesis, characterization, and receptor screening.

Molecular Pharmacology Fast Forward. Published on July 11, 2012 as DOI: 10.1124/mol.112.080291
This article has not been copyedited and formatted. The final version may differ from this version.

Figure Legends

Scheme 1. Generation of (1,4)-*anti* or (1,5)-*syn* 1,2,3-Triazoles with AChBP Template

Reactions performed with a biological template such as the AChBPs for synthesizing *in situ* compounds can potentially produce the (1,4)-*anti* or (1,5)-*syn* triazole products but separating the two was not possible by LCMS.

Scheme 2. Metal Catalyst Synthesis of Individual 1,2,3-Triazole Regioisomers

Experimental conditions for reactions performed with metal catalysts to produce each specific isomer of 1,2,3-triazole compounds (Cu(I) for (1,4)-*anti* and Ru(II) for (1,5)-*syn*).

Figure 1. Dose-Response Characterization of Triazoles with hα7-nAChR

Values were normalized as fractions to a max value of (±)-epibatidine obtained at either 100 nM or 60 nM. A, Characterization of (1,4)-*anti* triazoles (***1***-***5***) identified as agonists with triazole ***4*** found to have the highest potency with a rank order of ***4*** > ***5*** > ***2*** ≥ ***3*** ≥ ***1***. B, Quaternary tropane triazoles were found to be more potent agonists than the tertiary forms, rank order of $\boldsymbol{15}^{q} > \boldsymbol{4'} > \boldsymbol{22}^{q} > \boldsymbol{13}^{q} > \boldsymbol{16}^{t}$.

Figure 2. hα4β2-nAChR Competitive and Non-competitive Antagonist Profiles for Dihydro-beta-erythroidine (DHβE) and Mecamylamine.

Examples of competitive or non-competitive inhibition from concentration-response profiles produced with varying concentrations of (±)-epibatidine. A, Inhibited responses with DHβE produced classical competitive parallel shifts in EC_{50} values and were surmountable with increased agonist concentrations, both characteristic of predominantly competitive behavior (Competitive K_A = 300 ± 150 nM). Competitive K_A values were calculated from Schild plots using dose ratios and K_A = [A]/(DR-1). B, Mecamylamine inhibition produced minimal shifts in EC_{50} values with significant decreases in the max response indicative of predominantly non-competitive inhibition (Non-competitive K_A = 370 ± 60 nM).

Molecular Pharmacology Fast Forward. Published on July 11, 2012 as DOI: 10.1124/mol.112.080291
This article has not been copyedited and formatted. The final version may differ from this version.

Figure 3. hα4β2-nAChR Inhibition Profiles with *N*-methylammonium Tropane Quinolinone (1,4)-*anti* and (1,5)-*syn* triazole isomers (*4* and *4'*)

Concentration-response curves were generated with (±)-epibatidine in the presence and absence of identified antagonists produced inhibition constants and pharmacological profiles. A, The (1,4)-*anti* isomer ***4*** (K_A = 4 ± 2.9 μM) shows a potent competitive profile. B, (1,5)-*syn* isomer ***4'*** (K_A = 23 ± 5.6 μM) is less potent than the (1,4)-*anti* isomer.

Figure 4. Inhibition of Mouse 5-HT_{3A} with *N*-methylammonium Tropane Quinolinone (1,4)-*anti* and (1,5)-*syn* triazole isomers (*4* and *4'*)

A, Dose-response curves generated with 5-HT in the presence and absence of the quaternary tropane (1,5)-*syn* isomer ***4'*** that yielded competitive antagonism exemplified by parallel shifts in the EC_{50} values with increasing antagonist concentrations (K_A = 0.9 ± 0.4 μM). B, A Schild analysis of ***4'*** confirms competitive inhibition exhibited by a slope of -0.9. C, Confirmation of low activity with the (1,4)-*anti* isomer ***4***, calculated K_A = 34 ± 8.0 μM yielding a decrease in affinity of 38-fold compared to the (1,5)-*syn* counterpart.

Figure 5. Inhibition Profiles of Mouse 5-HT_{3A} Receptors with Compounds Generated *in situ* with *Ac*-MT2

Dose-response curves for 5-HT in the presence and absence of identified antagonists produced inhibition constants with slightly differing modes of inhibition. Each set of curves has an independent measurement of 5-HT concentration response without antagonist as reference curves (Hill slopes ranged from 2 to ~3). A, Competitive profiles were observed for triazoles ***13^t*** and ***22^t***. Competitive K_A values were 5 ± 1.4 μM and 12 ± 1.4 μM respectively. B, Mixed or non-competitive profiles were obtained for triazoles ***17^q*** and ***18^t***. Non-competitive K_A values were 8 ± 1.1 μM and 14 ± 3.2 μM respectively.

Molecular Pharmacology Fast Forward. Published on July 11, 2012 as DOI: 10.1124/mol.112.080291
This article has not been copyedited and formatted. The final version may differ from this version.

Figure 6. Crystallographic Poses of Triazole *4* (Quaternary Tropane) Overlaid with Tropisetron (Tertiary Tropane), Nicotine, and Epibatidine Complexes with *Ac* and *Ls*-AChBPs

A. Primary face and B. complementary face residues from overlaid structures of Triazole ***4*** **(**PDB ID: 4DBM) in cyan, referred to as ***18*** in (Grimster et al., 2012), and tropisetron (PDB ID: 2WNC) in mustard (Hibbs et al., 2009) both in complex with *Ac*-AChBP. Respective residues shown in stick form are within 4Å of respective ligands, green for triazole ***4*** and orange for tropisetron. Polar contacts for each ligand are shown colored accordingly with an additional representation of the distance from the quaternary nitrogen in ***4*** to the backbone carbonyl of Trp 147 indicating proximity and potential cation-π interaction with the aromatic indole side chain. C. Additional ligand overlay of complexes including nicotine (plum) in *Ls*-AChBP (magenta) (Celie et al., 2004) and epibatidine (salmon) in *Ac*-AChBP (beige) (Hansen et al., 2005) PDB IDs 1UW6 and 2BYQ respectively. Triazole ***4*** and tropisetron colored according to A and B. Distances of nitrogen atom are shown and compared between quaternary tropane of ***4***, tertiary tropane of tropisetron, pyrolidine of nicotine, and azabicyloheptane of epibatidine to backbone carbonyl oxygen of Trp 147. A hydrogen bond between the N3 atom of triazole ***4*** and a water (red sphere) is comparable to the hydrogen bond of water (magenta sphere) and the pyridine ring of nicotine. Shown below the panels is a sequence alignment of the relevant residues (and interconnecting residues) listed in each subunit. Blue highlighted residues are conserved aromatic residues in the primary subunit (loops A, B, and C). Red highlighted residues are changes in the 5-HT_{3A} primary subunit, in which two key aromatic residues are lost compared to *Ac*-AChBP and nAChRs (Tyr 93 and Tyr 188). Purple highlighted residues are changes in the 5-HT_{3A} complementary subunit (loops D and E), which substitutes aromatic tyrosine residues at 106, 108, and 118 not found in *Ac*-AChBP and nAChRs.

Molecular Pharmacology Fast Forward. Published on July 11, 2012 as DOI: 10.1124/mol.112.080291
This article has not been copyedited and formatted. The final version may differ from this version.

Table 1. Receptor and AChBP Activities of *in situ* Leads Generated with *Ac* and *Ls*-AChBPs (A.) Cyclic Quaternary Amine-Quinolinone (1,4)-*anti* and (1,5)-*syn* Triazoles, (B.) Quaternary Tropane (1,4)-*anti* Triazoles with Various Aromatic Groups Attached via the Alkyne Building Block

Compilation of receptor functional activity (human α7-nAChR, human α4β2-nAChR, and mouse 5-HT_{3A} receptors) and AChBP dissociation constants of compounds generated *in situ* on wt *Ls*, *Ac*, and *Ac*-Y55W AChBPs (***1-5***, ***1'-5'***, ***6-9***). *AChBP dissociation constants were calculated from the SPA competition assay with [H^3]-(±)-epibatidine, structure and AChBP binding properties of compounds ***1-9*** and ***4'*** were previously reported in (Grimster et al., 2012). Competitive (C) and non-competitive (NC) antagonist values. †Antagonism of α4β2-nAChRs showed mixed inhibition but non-competitive antagonist values were greater by factors of 1.3-20, hence inhibition was primarily competitive (both C and NC values are shown in Supplemental Table 2). Compounds with values represented as > 30 μM were not identified as antagonists from screens (Supplemental Figure 1). All values are reported as means ± S.D. with (n) experiments. Counter ions shown as $\mathbf{X}^-$ in chemical structures differ between isomers and are listed in Supplemental Table 7. The full molecular structures for ***4*** and ***4'*** are shown in Figures 3 and 4.

Molecular Pharmacology Fast Forward. Published on July 11, 2012 as DOI: 10.1124/mol.112.080291
This article has not been copyedited and formatted. The final version may differ from this version.

Table 1A Quinolinone Triazoles 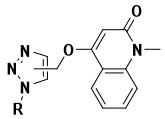		**EC_{50}, μM** Agonists	**K_A, μM** Antagonists		**K_d, nM** Binding AChBPs*		
Azide R Groups		**hα7**	**hα4β2†**	**m5-HT_{3A}**	***Ls***	***Ac***	***Ac*Y55W**
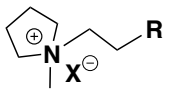	(*1*) *anti*	3.7 ± 0.79 (5)	20 ± 11 (3) C	> 30	18 ± 3.0 (3)	540 ± 77 (3)	62 ± 9.0 (3)
	(*1'*) *syn*	6 ± 2.3 (6)	30 ± 13 (3) C	> 30	60 ± 10 (3)	1400 ± 370 (3)	170 ± 30 (3)
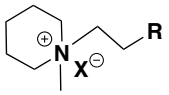	(*2*) *anti*	1.2 ± 0.65 (6)	12 ± 5.6 (3) C	> 30	10 ± 1.7 (3)	210 ± 46 (3)	50 ± 5.0 (3)
	(*2'*) *syn*	4.2 ± 0.81 (6)	> 30 (3)	> 30	40 ± 15 (3)	800 ± 210 (3)	210 ± 60 (3)
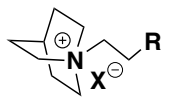	(*3*) *anti*	1.8 ± 0.96 (4)	8 ± 1.8 (3) C	> 30	9.0 ± 0.4 (3)	120 ± 25 (3)	88 ± 4.2 (3)
	(*3'*) *syn*	2.9 ± 0.58 (7)	30 ± 13 (3) C	> 30	24 ± 5.4 (3)	250 ± 80 (3)	290 ± 85 (3)
	(*4*) *anti*	0.3 ± 0.16 (6)	4 ± 2.9 (3) C	34 ± 8.0 (3) C	1.0 ± 0.22 (3)	24 ± 6.8 (3)	17 ± 4.8 (3)
	(*4'*) *syn*	0.6 ± 0.12 (5)	23 ± 5.6 (6) C	0.9 ± 0.40 (4) C	2 ± 1.0 (3)	300 ± 110 (3)	100 ± 36 (3)
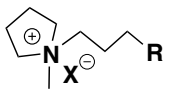	(*5*) *anti*	0.8 ± 0.19 (6)	18 ± 8.8 (3) C	> 30	80 ± 14 (3)	470 ± 65 (3)	280 ± 21 (3)
	(*5'*) *syn*	2.0 ± 0.37 (6)	40 ± 18 (3) C	> 30	600 ± 140 (3)	1400 ± 480(3)	800 ± 210 (3)
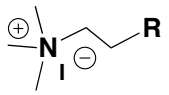	(*6*) *anti*	1.7 ± 0.82 (6)	14 ± 9.7 (3) C	> 30	80 ± 26 (3)	1900 ± 800 (3)	370 ± 50 (3)

Table 1B		**EC_{50}, μM** Agonists	**K_A, μM** Antagonists		**K_d, nM** Binding AChBPs*		
Triazole #		**hα7**	**hα4β2†**	**m5-HT_{3A}**	***Ls***	***Ac***	***Ac*Y55W**
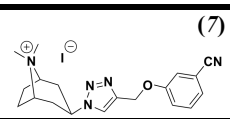	(*7*)	0.9 ± 0.38 (3)	> 30	> 30	40 ± 19 (3)	220 ± 87 (3)	130 ± 35 (3)
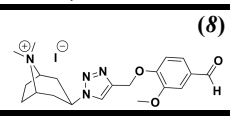	(*8*)	1.0 ± 0.45 (3)	6 ± 2.9 (4) C	> 30	60 ± 26 (3)	260 ± 80 (3)	130 ± 44 (3)
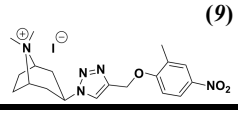	(*9*)	1.9 ± 0.54 (4)	14 ± 8.9 (3) C	> 30	13 ± 6.5 (3)	60 ± 27 (3)	30 ± 18 (3)

Molecular Pharmacology Fast Forward. Published on July 11, 2012 as DOI: 10.1124/mol.112.080291
This article has not been copyedited and formatted. The final version may differ from this version.

Table 2. Receptor Activities of *N*-methylammonium Tropane (1,4)-*anti* Triazoles (*10*^{q}-*23*^{q}) Generated *in situ* with α7-AChBP Partial Chimera (*Ac*-MT2)

All reported values are means ± S.D. with (n) experiments. Competitive (C) and non-competitive (NC) values. Compounds with values represented as > 30 μM for receptors were not identified from either receptor screens (Supplemental Figure 4), nor were values represented as > 5000 nM found to bind AChBPs (data not shown).

Quaternary (^{q}) Tropane (1,4)-*anti* Triazoles 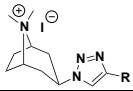	EC_{50}, μM Agonists	K_A, μM Antagonists		K_d, nM Binding AChBPs			
Alkyne R Groups	**hα7**	**hα4β2**	**m5-HT$_{3A}$**	***Ls***	***Ac***	***Ac*Y55W**	***Ac*-MT2**
(*4*) 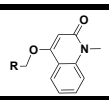	0.3 ± 0.16 (6)	4 ± 2.9 (3) C 60 ± 13 (3) NC	34 ± 7.8 (3) C	1.0 ± 0.22 (3)	24 ± 6.8 (3)	17 ± 4.8 (3)	40 ± 17 (3)
(*10*^{q}) 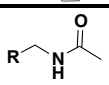	5 ± 3.0 (7)	> 30	> 30	> 5000	800 ± 310 (3)	> 5000	900 ± 150 (3)
(*11*^{q}) 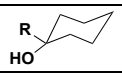	9 ± 2.0 (4)	> 30	> 30	> 5000	> 5000	> 5000	50 ± 19 (3)
(*12*^{q}) 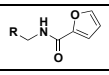	3 ± 1.8 (9)	> 30	> 30	400 ± 190 (4)	600 ± 260 (3)	1000 ± 150 (3)	700 ± 270 (3)
(*13*^{q}) 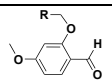	0.8 ± 0.46 (11)	7 ± 2.8 (4) C 19 ± 4.4 (4) NC	> 30	20 ± 16 (3)	110 ± 30 (3)	120 ± 70 (3)	80 ± 24 (3)
(*14*^{q}) 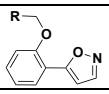	2 ± 1.0 (7)	> 30	> 30	50 ± 15 (3)	140 ± 74 (3)	170 ± 85 (3)	96 ± 8.5 (3)
(*15*^{q}) 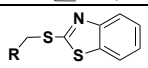	0.20±0.068 (10)	3 ± 1.7 (4) C 8 ± 3.8 (4) NC	> 30	4 ± 1.3 (3)	13 ± 6.9 (3)	13 ± 4.4 (3)	8 ± 1.1 (3)
(*16*^{q}) 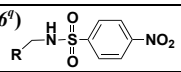	1.8 ± 0.85 (8)	> 30	> 30	> 5000	620 ± 94 (3)	800 ± 420 (3)	600 ± 180 (3)
(*17*^{q}) 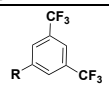	0.9 ± 0.25 (9)	5 ± 2.4 (4) C 5 ± 2.0 (4) NC	50 ± 14 (3) C 8 ± 1.1 (3) NC	130 ± 62 (3)	110 ± 20 (3)	300 ± 140 (3)	400 ± 100 (3)
(*18*^{q}) 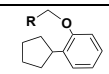	0.4 ± 0.28 (9)	4 ± 1.3 (5) C 8 ± 3.0 (5) NC	> 30	70 ± 32 (3)	260 ± 52 (3)	270 ± 54 (3)	440 ± 89 (3)
(*19*^{q}) 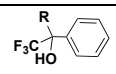	2 ± 1.1 (8)	22 ± 4.7 (4) C 41 ± 7.2 (4) NC	> 30	120 ± 29 (3)	800 ± 460 (3)	> 5000	60 ± 27 (3)
(*20*^{q}) 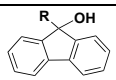	4 ± 2.5 (10)	15 ± 5.7 (5) C 23 ± 5.6 (5) NC	> 30	50 ± 28 (3)	400 ± 100 (3)	600 ± 280 (4)	120 ± 48 (3)
(*21*^{q}) 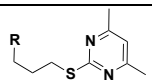	3 ± 1.4 (9)	60 ± 32 (2) C 27.1 ± 0.19 (2) NC	> 30	40 ± 18 (3)	18 ± 7.8 (3)	30 ± 17 (3)	400 ± 110 (3)
(*22*^{q}) 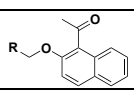	0.4 ± 0.22 (10)	> 30	> 30	160 ± 57 (3)	200 ± 82 (3)	300 ± 150 (3)	900 ± 260 (3)
(*23*^{q}) 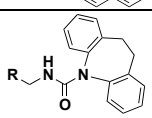	8 ± 3.6 (9)	30 ± 21 (4) C 40 ± 18 (4) NC	> 30	500 ± 200 (3)	420 ± 43 (3)	1000 ± 300 (3)	2000±700 (3)

Molecular Pharmacology Fast Forward. Published on July 11, 2012 as DOI: 10.1124/mol.112.080291
This article has not been copyedited and formatted. The final version may differ from this version.

Table 3. Functional Activity of Receptors and Dissociation Constants of AChBPs with Tertiary Tropane (1,4)-*anti* Triazole Analogues (*4*^{t}, *10*^{t}-*23*^{t}) Generated by Cu(I) Catalysis

All reported values are means ± S.D. with (n) experiments. Competitive (C) and non-competitive (NC) values. Compounds with values represented as > 30 μM for receptors were not identified from either receptor screens (Supplemental Figure 4), nor were values represented as > 5000 nM found to bind AChBPs (data not shown).

Tertiary (^{t}) Tropane (1,4)-*anti* Triazoles 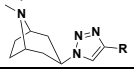	EC_{50}, μM Agonists	K_A, μM Antagonists		K_d, nM Binding AChBPs			
Alkyne R Groups	**hα7**	**hα4β2**	**m5-HT$_{3A}$**	***Ls***	***Ac***	***Ac*Y55W**	***Ac*-MT2**
(*4*^{t}) 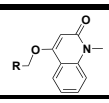	11 ± 6.1 (5)	14 ± 9.7 (3) C	15 ± 1.5 (3) C	1.30 ± 0.011 (3)	109 ± 2.8 (3)	16 ± 1.7 (3)	600 ± 150 (3)
(*10*^{t}) 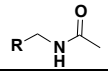	> 30	18 ± 8.3 (3) C 29 ± 3.7 (3) NC	> 30	900 ± 120 (3)	> 5000	> 5000	> 5000
(*11*^{t}) 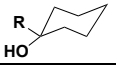	> 30	> 30	> 30	> 5000	> 5000	> 5000	> 5000
(*12*^{t}) 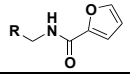	> 30	30 ± 19 (3) C 20 ± 11 (3) NC	> 30	210 ± 78 (3)	> 5000	1400 ± 520 (3)	> 5000
(*13*^{t}) 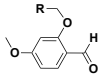	> 30	20 ± 15 (4) C 6 ± 3.8 (5) NC	5 ± 1.4 (3) C	26 ± 8.2 (3)	1200 ± 360 (3)	390 ± 49 (3)	> 5000
(*14*^{t}) 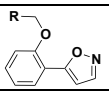	> 30	16 ± 9.0 (4) C 13 ± 5.2 (4) NC	> 30	25 ± 4.1 (3)	500 ± 210 (3)	300 ± 120 (3)	> 5000
(*15*^{t}) 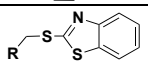	12 ± 2.1 (3)	8 ± 6.5 (2) C 4 ± 2.8 (3) NC	32 ± 8.5 (3) C	40 ± 16 (3)	240 ± 82 (3)	140 ± 59 (3)	110 ± 48 (3)
(*16*^{t}) 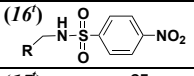	5 ± 1.8 (4)	60 ± 27 (3) C 30 ± 16 (5) NC	> 30	> 5000	> 5000	> 5000	> 5000
(*17*^{t}) 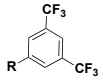	> 30	> 30	> 30	600 ± 190 (3)	1100 ± 270 (3)	> 5000	> 5000
(*18*^{t}) 	> 30	5 ± 1.8 (4) C 3 ± 1.8 (4) NC	12 ± 2.8 (3) C 14 ± 3.2 (3) NC	30 ± 7.7 (3)	900 ± 220 (3)	370 ± 50 (3)	> 5000
(*19*^{t}) 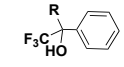	> 30	80 ± 53 (3) C 40 ± 21 (3) NC	> 30	> 5000	> 5000	> 5000	> 5000
(*20*^{t}) 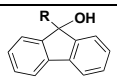	12 ± 6.1(3)	17 ± 7.5 (3) C 39 ± 2.0 (3) NC	> 30	500 ± 200 (4)	2000 ± 130 (3)	3100 ±460 (3)	> 5000
(*21*^{t}) 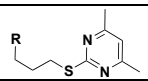	> 30	10 ± 12 (3) C 20 ± 10 (3) NC	> 30	300 ± 110 (3)	360 ± 40 (3)	560 ± 80 (3)	> 5000
(*22*^{t}) 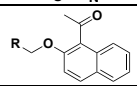	9 ± 1.1 (3)	5 ± 2.5 (5) C 4 ±1.6 (5) NC	12 ± 1.4 (3) C	141 ± 8.3 (3)	800 ± 120 (3)	700 ± 100 (3)	> 5000
(*23*^{t}) 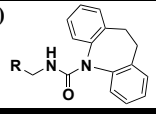	> 30	20 ± 5.7 (2) C 13 ±4.3 (3) NC	> 30	> 5000	1300 ± 400 (3)	1020 ± 72 (3)	> 5000

Scheme 1

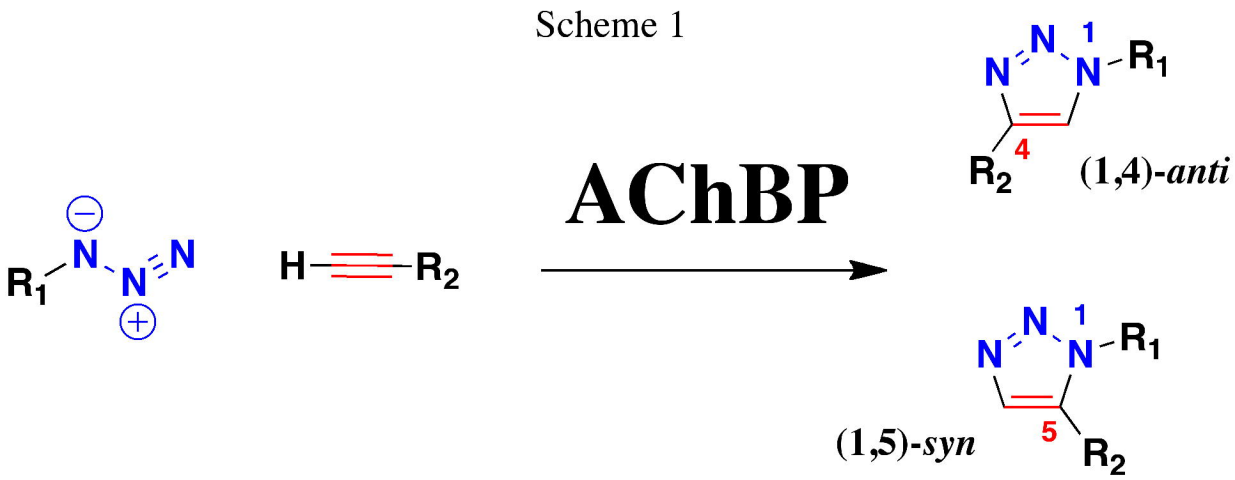

Scheme 2

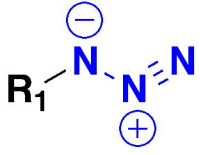

CuAAC

1mol% $CuSO_4$-$5H_2O$
10 mol% Na ascorbate

20°C, 1-48hrs
1:1 H2O/tBuOH

(1,4)-*anti*

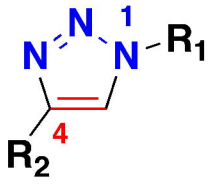

3% $Cp^*RuCl(PPh_3)_2$
dioxane

60°C, 4-8hrs

RuAAC

(1,5)-*syn*

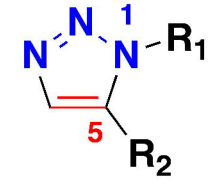

Figure 1

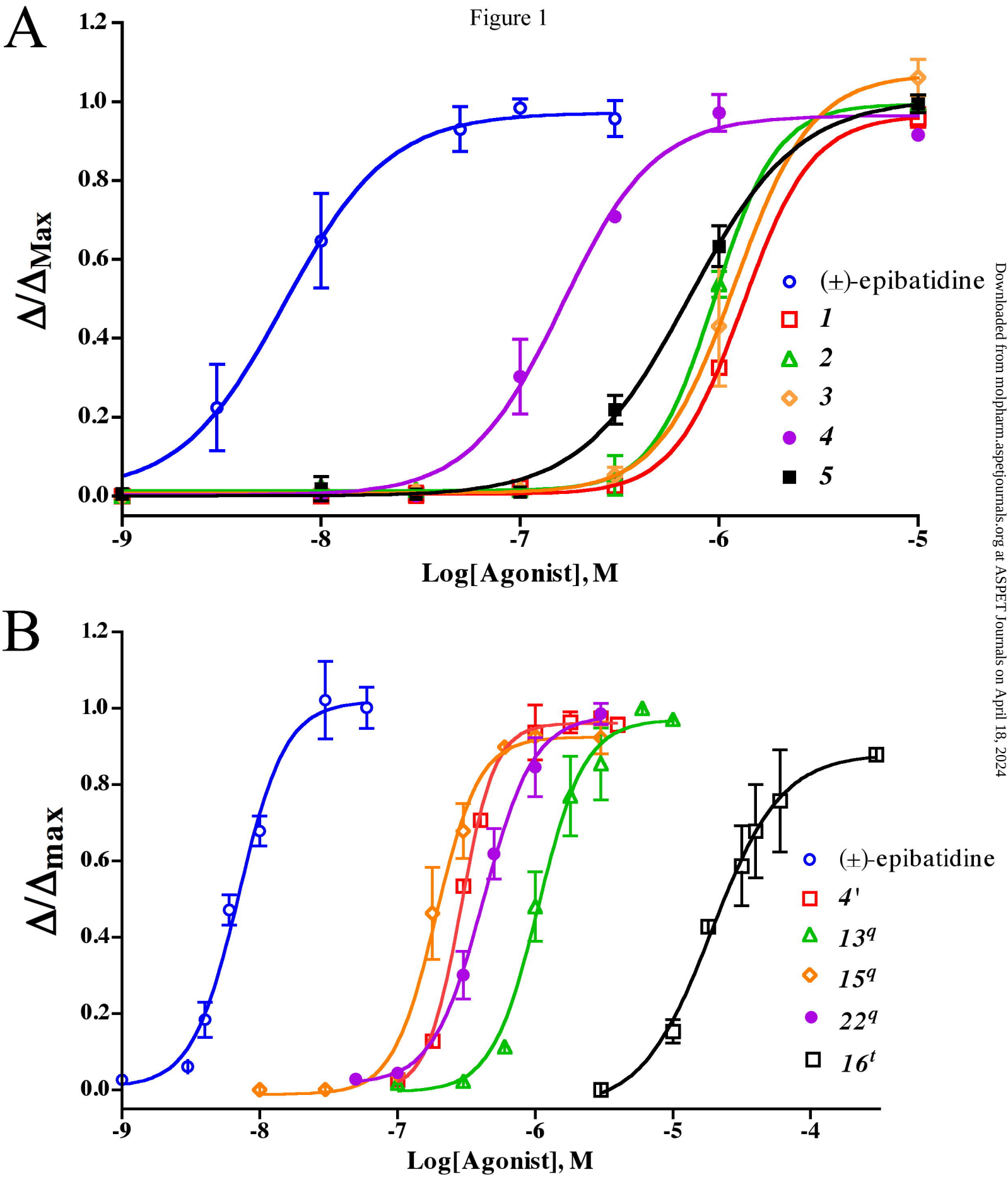

Figure 2

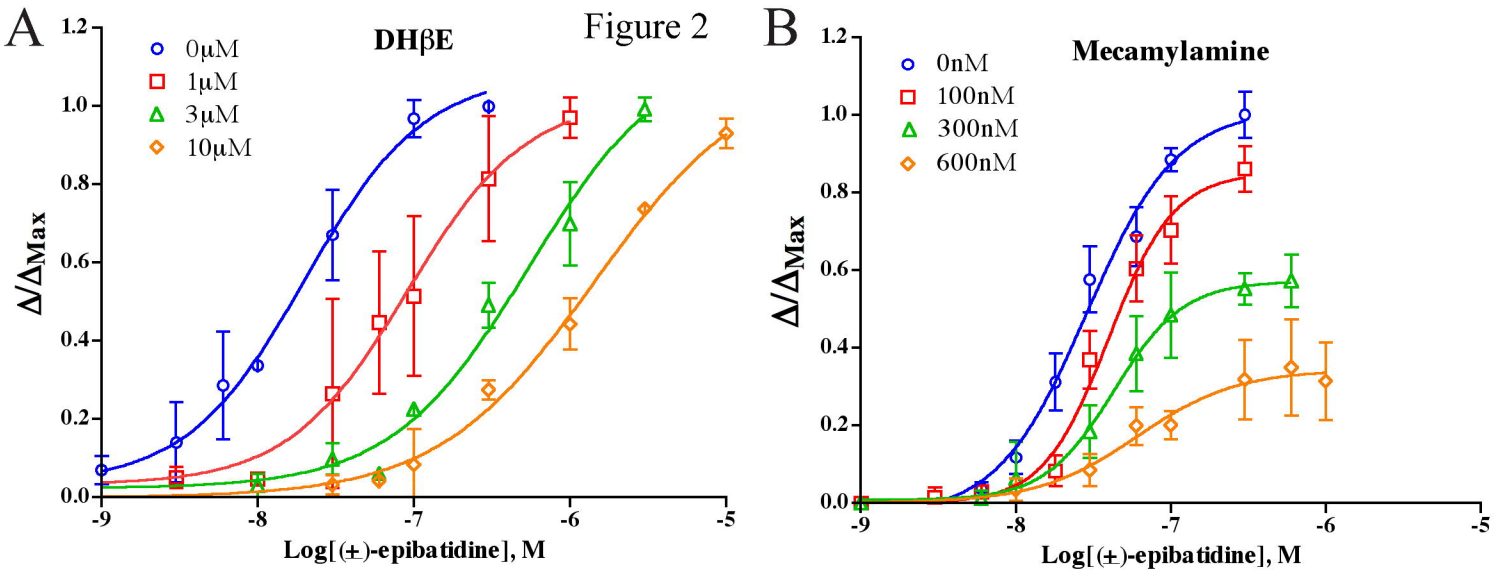
A
DHβE
0μM
1μM
3μM
10μM
Δ/Δ_Max
1.2
1.0
0.8
0.6
0.4
0.2
0.0
-9
-8
-7
-6
-5
Log[(±)-epibatidine], M
B
Mecamylamine
0nM
100nM
300nM
600nM
Δ/Δ_Max
1.2
1.0
0.8
0.6
0.4
0.2
0.0
-9
-8
-7
-6
-5
Log[(±)-epibatidine], M

Figure 3

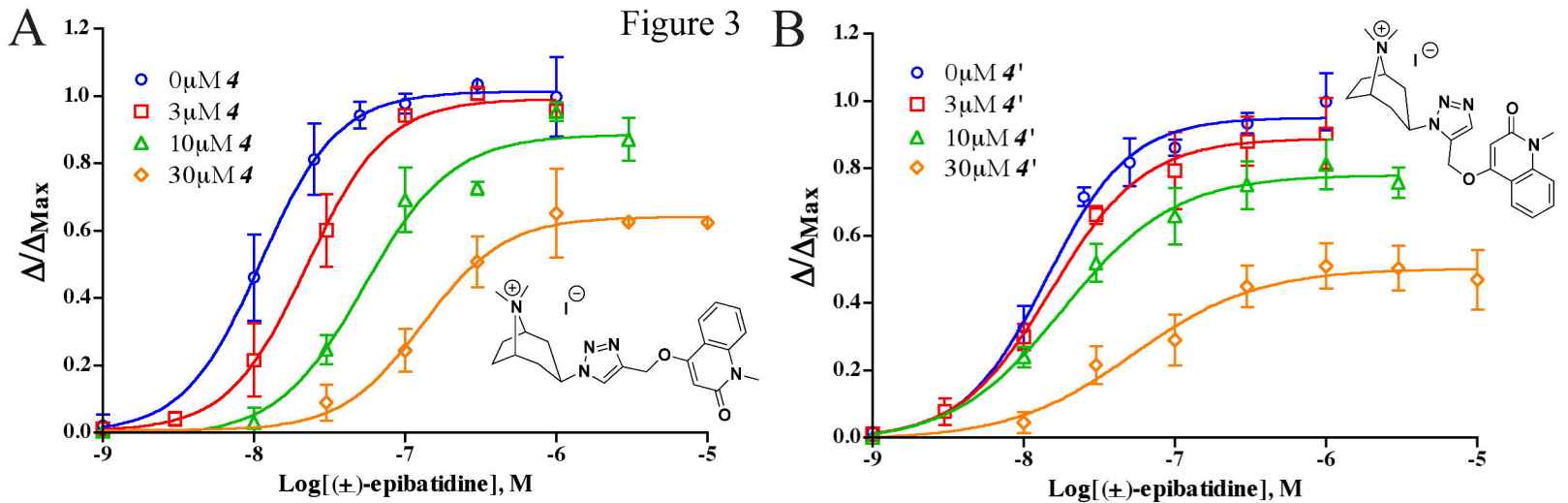
A
B
0μM 4
3μM 4
10μM 4
30μM 4
0μM 4'
3μM 4'
10μM 4'
30μM 4'
Δ/ΔMax
Log[(±)-epibatidine], M
1.2
1.0
0.8
0.6
0.4
0.2
0.0
-9
-8
-7
-6
-5
N
I
N=N
O

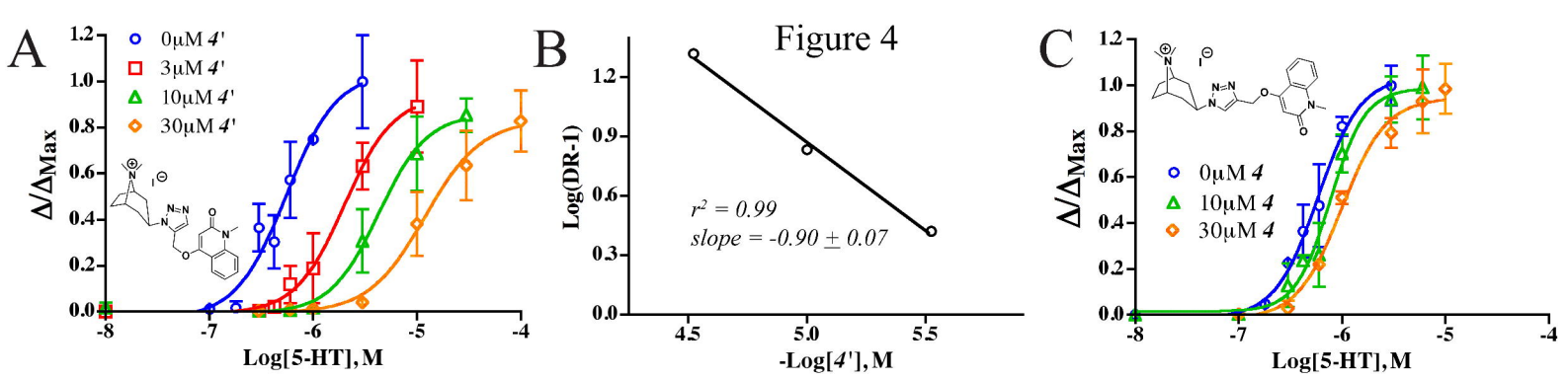
A
0μM 4'
3μM 4'
10μM 4'
30μM 4'
Δ/ΔMax
Log[5-HT],M
B
Figure 4
Log(DR-1)
r² = 0.99
slope = -0.90 ± 0.07
-Log[4'],M
C
0μM 4
10μM 4
30μM 4
Δ/ΔMax
Log[5-HT],M

Figure 5

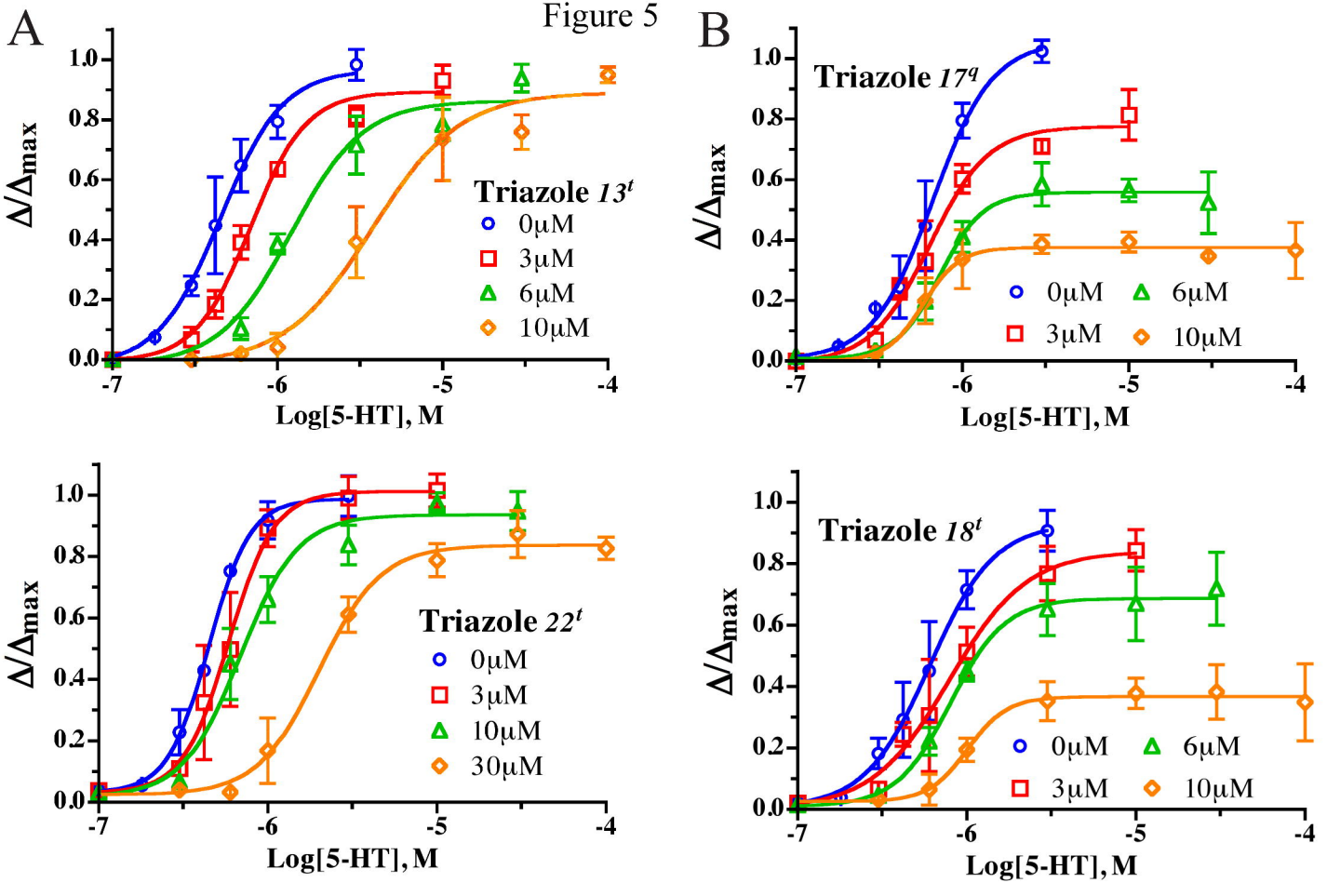
A
B
Triazole 13t
0μM
3μM
6μM
10μM
Triazole 17q
Triazole 22t
30μM
Triazole 18t
Δ/Δmax
Log[5-HT], M

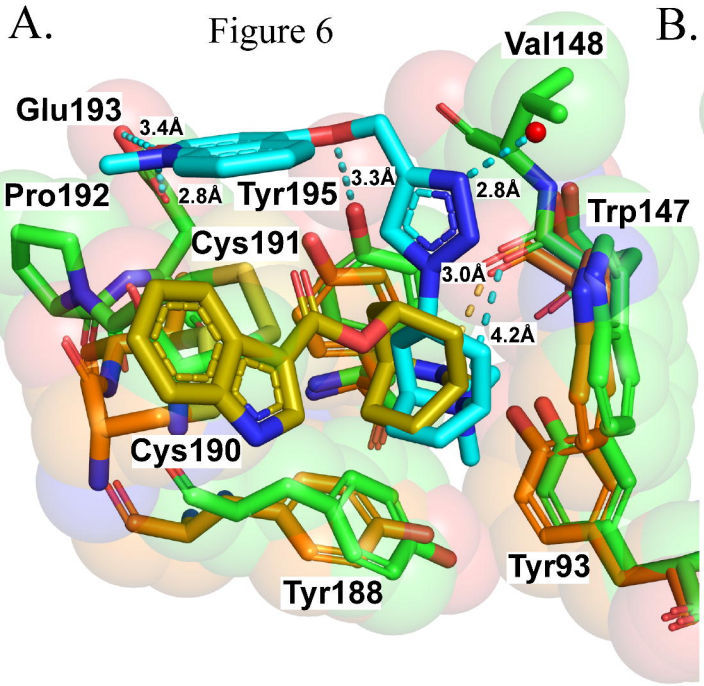

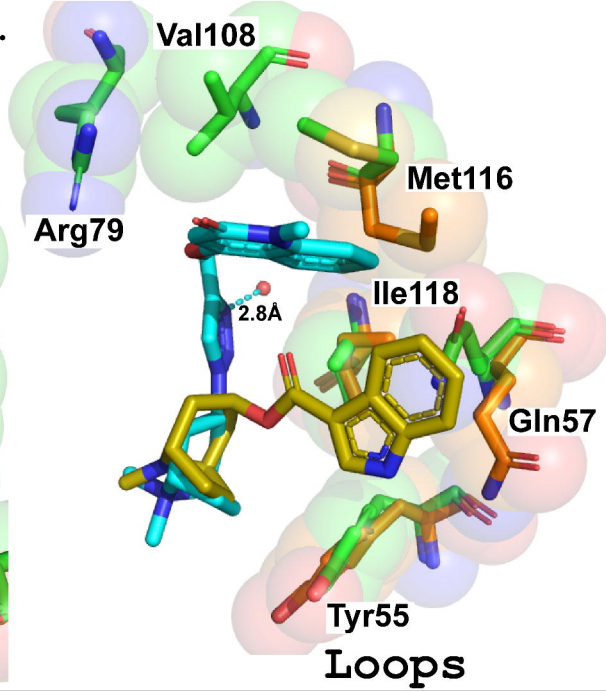

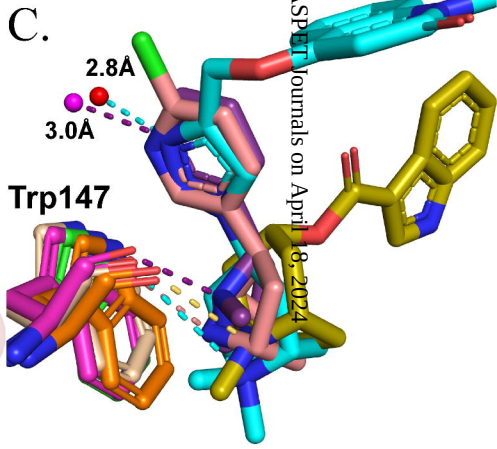

Distance from N to backbone carbonyl oxygen of Trp 147

nicotine	2.8Å
tropisetron	3.0Å
epibatidine	3.0Å
triazole 4	4.2Å

Loops

	D		A	E		B	C
	55...	79...	93...	106...	116...	146...	188...
Aplysia californica	YEQ...	R...	Y...	IAV...	MFI...	SWVYSG...	YSCCPEPY..
hα7	WLQ...	R...	Y...	NVL...	QYL...	SWSYGG...	YECCKEPY..
hα4			Y...			SWTYDK...	YECCAEIY..
hβ2	WLT...	R...		NAV...	FWL...		
m5-HT$_{3A}$	WYR...	S...	N...	YVY...	QNY...	SWLHTI...	IDI-SNSY..